

**Ecophysiological response of Chilean  
*Desmophyllum dianthus* to  
Mediterranean environmental  
conditions**

Master thesis

By Sophia Kleemeier

Supervisors: Dr. Jürgen Laudien  
Dr. Covadonga Orejas

## Executive summary

The cosmopolitan cold-water coral *Desmophyllum dianthus* is an important ecosystem engineer, providing habitat for many benthic organisms and thus supporting high local biodiversity (Roberts *et al.*, 2009; Häussermann *et al.*, 2021). Although most CWC populations are located in the bathyal zones of the oceans, few *D. dianthus* populations have spread to the depths of the Mediterranean Sea, representing one of the most saline marine habitats on earth. Other populations at higher latitudes, such as in the Chilean fjord system, settle already in shallow waters as part of a deep-water emerging benthic fauna (Försterra *et al.*, 2016) and are therefore exposed to natural fluctuations in abiotic and biotic environmental parameters (Försterra and Häussermann, 2003; Försterra *et al.*, 2005; Risk *et al.*, 2002). In particular, changes in temperature and salinity affect physiological processes of CWCs. Thus, the aim of this study was to explore the potential capability of *D. dianthus* to thrive in environments with different physical and chemical water parameters, as a result of its capability to acclimate in a short time to changing environmental conditions. To this end, the response of *D. dianthus* specimens from Chilean populations to an elevated temperature and salinity to which the populations in the Mediterranean Sea are exposed was investigated. A uni- and bifactorial approach was used to identify the single effect of increased temperature and the synergistic effect of increased temperature and salinity on polyp behavior, respiration rate, and growth. While both, warming alone and in combination with increased salinity, did not affect behavior nor respiration, increased temperature in combination with increased salinity stimulated the growth of *D. dianthus* by 140 %. This increase very likely results from the positive correlation of growth with aragonite saturation, which forms the basis for the coral calcification process (Morse *et al.*, 2007). The effect of salinity in promoting growth of calcifying marine invertebrates up to a species-specific threshold was already observed (Ries *et al.*, 2009). In conclusion, Chilean *D. dianthus* specimens are capable of surviving and growing significantly more under higher temperature and salinity, corresponding to the ones documented in the Mediterranean Sea, for a period of three months. This indicates that Chilean *D. dianthus* specimens are plastic and resistant and consequently its widespread distribution might likely be due to this great phenotypic plasticity with respect to different physical and chemical characteristics of the water masses.

## Abstract

The cold-water coral *Desmophyllum dianthus* thrives in mostly oceans of the world and is thus one of the most widespread scleractinians. Since the environmental conditions in the various habitats this coral inhabits differ greatly, the question arises whether the distribution is mainly evolutionary (adaptation to different environmental conditions) or whether the species has a high acclimation potential that enables it to colonize new habitats in a relatively short time. To test the acclimation potential (phenotypic plasticity), *D. dianthus* specimens from Chilean Comau Fjord were exposed to conditions prevailing in the Mediterranean Sea. Using an uni- and bifactorial approach, I tested the single effect of elevated temperature (12 °C) and the interactive effect of elevated temperature and salinity (38 [PSU scale]) on polyp expansion, respiration, and growth of the corals. While polyp expansion, as well as respiration rates, were not affected by the increase in temperature and by its combination with high salinity, an increase in growth of 140 % was recorded, stimulated by increased salinity and the associated increased aragonite saturation. Consequently, the species has a great phenotypic plasticity, which explains the cosmopolitan distribution of *D. dianthus*.

## 1 Introduction

Scleractinian cold-water corals (CWCs) are mainly located in cold and temperate marine habitats and are important ecosystem engineers by constructing complex bioherms and reefs throughout the world's oceans (Freiwald *et al.*, 2004; Roberts *et al.*, 2006, 2009; Wild *et al.*, 2008; Büscher *et al.*, 2017). By providing structural habitat for diverse benthic species communities, CWCs support hot spots of biodiversity in marine ecosystems (Roberts *et al.*, 2009). In addition to providing structural habitats, CWCs play an important role in marine biogeochemical cycles, promoting mass and energy transfer between pelagic and benthic systems (Gili and Coma, 1998; Van Oevelen *et al.*, 2009), through the sequestration of organic carbon, which is assimilated in the form of detritus, phyto- and zooplankton (Duineveld *et al.*, 2004; 2007, 2012; Carrier *et al.*, 2009; Dodds *et al.*, 2009).

### 1.1 Biogeochemical seawater parameters and their impact on scleractinian CWCs

The occurrence of CWCs is influenced by various biotic and abiotic environmental factors, such as food and settling substrate availability, oxygen saturation, aragonite saturation, temperature, and salinity (Cairns and Parker, 1992; Guinotte *et al.*, 2006; Thiem *et al.*, 2006; Roberts *et al.*, 2006, 2009; Miensis *et al.*, 2007; White *et al.*, 2007; Cairns, 2007; Dullo *et al.*, 2008; Davies *et al.*, 2009). As the distribution and abundance of CWCs depend on environmental conditions,

CWCs currently face threats from global climate change, to which they must genetically adapt or acclimatize to maintain local populations (Coles, 1978; Hoegh-Guldberg *et al.*, 2007; Hoegh-Guldberg, 2014).

## 1.2 Seawater temperature modulating CWC occurrence

Seawater temperature is one of the most important environmental factors, strongly affecting CWCs' physiological processes (Clausen and Roth, 1975; Buddemeier and Kinzie, 1976; Coles and Jokiel, 1977; Howe and Marshall, 2002; Dodds *et al.*, 2007; Naumann *et al.*, 2014) and thus controlling corals' occurrence in worlds' oceans (Freiwald *et al.*, 2009; Roberts *et al.*, 2009). Most studies focused only on the effects of single stressors to determine e.g., species-specific thermal thresholds (e.g., Naumann *et al.*, 2013; Chapron *et al.*, 2021). Studies on Mediterranean CWCs, which were assumed to already live at their upper thermal limit (Freiwald *et al.*, 2009; Brooke *et al.*, 2013), revealed varying thermal tolerance ranges (Naumann *et al.* 2011, 2013, 2014; Gori *et al.* 2014). *D. dianthus* and *M. oculata* showed no physiological alterations to temperatures of 17 °C and 17.5 °C, respectively, which is already close to the temperature range of some temperate corals, whereas the metabolism of the CWC *Desmophyllum pertusum* (syn. *Lophelia pertusa*; Addamo *et al.*, 2015) living in the same habitat is already negatively affected at 15 °C (Naumann *et al.*, 2013; Chapron *et al.*, 2021). Thus, some Mediterranean CWC species tolerate elevated ambient temperatures, at least temporarily, indicating that not all species may currently be living at their upper thermal limits, which could threaten their survival as warming progresses (Castric-Fey, 1997; Palanques *et al.*, 2006; Freiwald *et al.*, 2009). Understanding the sensitivity of CWCs to ocean warming by identifying species-specific thresholds in different geographical areas helps to understand the threat to corals and their associated communities from climate change at local and global scale.

However, as climate change affects multiple seawater parameters simultaneously, multifactorial laboratory studies offer more realistic predictions of the physiological responses of corals. The synergistic effects on the physiological capability of CWCs to cope with multiple altered environmental factors are not well understood, as the responses are more complex than the coral performance found in unifactorial experiments (Hofmann and Todgham, 2010). In most multifactorial experiments, the effect of ocean warming is often simulated and analyzed in combination with additional altered abiotic or biotic factors. In particular, the effects of increasing temperature and alteration of seawater carbonate chemistry on calcifying organisms have already been well studied for many tropical (e.g., Muehllehner and Edmunds, 2008; Hoegh-Guldberg *et al.*, 2017) and CWCs (e.g., Gori *et al.*, 2014, 2016; Büscher *et al.*, 2017).

### 1.3 Salinity modulating CWC occurrence

Although corals also suffer from osmotic stress, the capacities of tropical corals and CWCs in particular, to withstand alterations in seawater salinity is not as well studied as thermal thresholds. Similar to temperature, the tolerance to osmotic stress, driven by dynamic variability of ambient environmental conditions is species-specific (Coles, 1992) and has been already studied for tropical corals (e.g., Moberg *et al.*, 1997; Lirman and Manzello, 2009; Faxneld *et al.*, 2010; Berkelmans *et al.*, 2012; Dias *et al.*, 2019a, b).

#### 1.3.1 Osmoregulation strategies and their limitations

To perform efficient metabolic processes, all organisms require optimal intracellular conditions and are therefore sensitive to extreme alterations in the concentration of osmotic active molecules (osmolytes) caused by salinity variations. Marine species in particular face the problem of finding the balance between the energetic cost of maintaining intracellular osmolyte concentrations and the optimal functionality of metabolic activity, and consequently developed two main strategies during evolution. Marine vertebrates perform osmoregulation, whereas most marine invertebrates are osmoconformers. The osmoregulation strategy is based on maintaining the optimal intracellular concentration of osmolyte for metabolic activity, regardless of a deviating extracellular concentration (Mayfield and Gates, 2007). Due to continuous active ion transports, species that engage in osmoregulation must invest more energy than species that engage in osmoconformation (Somero and Yancey, 1997), which can become energetically unfavorable if external osmolarity exceeds or falls below species-specific salinity thresholds (Coles, 1992, Hochachka and Somero, 2002). Marine invertebrates, like corals, have limited capacity to regulate the cells' internal osmotic pressure, which therefore fluctuates according to the external osmolarity (Florkin, 1962). Since these species invest less energy in the osmoregulatory process, osmoconformation is an energetically favourable strategy (Coles and Jokiel, 1992; Manzello and Lirman, 2003). Prolonged osmotic stress can expose these organisms to extreme concentrations of inorganic ions that limit enzymatic functions, leading to dysfunction of various organelles (Lang, 1998; Oren, 1999). In addition, fluctuations in internal osmolyte concentrations can result in increased production of reactive oxygen species (ROS) that impair cellular metabolism (Ballantyne and Moon, 1986; Shivakumar and Jayaraman, 1986). Consequently, hyper- and hypotension in the cell lead to fluctuations in intracellular water volume, which can manifest as cell shrinkage or expansion and can mechanically damage the cytoskeleton and membrane structures (Maeda and Thompson, 1986;

Jahnke and White, 2003; Mayfield and Gates, 2007). Therefore, changes in salinity can negatively affect coral physiology, such as feeding rate, metabolic activity, excretion (Normant and Lamprecht, 2006), growth, and reproductive success (Coles and Jokiel, 1992; Humphrey *et al.*, 2008; Flaxneld *et al.*, 2010), and can lead to mortality (Coles and Jokiel, 2018).

#### 1.4 The synergetic effect of temperature and salinity

Most studies regarding increased temperature and decreased salinity have been conducted on reef-building tropical corals that are threatened by freshwater runoff, heavy rainfall, tidal activities, and ocean warming due to their predominant distribution in coastal areas (Crossland, 1928; Gorea, 1964; Coles and Jokiel, 1978; Jokiel *et al.*, 1993; van Woesik *et al.*, 1995; Xiubao *et al.*, 2009; Faxneld *et al.*, 2010; Dias *et al.*, 2019a, b). The observed synergistic effect of altered thermal and osmotic conditions is often the result of a strong increase in metabolic activity due to elevated temperature described by the Q10 rule (Van't Hoff, 1886) and the energetic costs of cellular activities occurring under unfavorable osmotic conditions (Dias *et al.*, 2019a, b).

Besides alterations in metabolic activities, growth of the tropical scleractinian corals *Montipora verrucosa* and *Gonipora columna* was reduced (Coles and Jokiel, 1978; Ding *et al.*, 2022). Furthermore, reduced salinity and elevated temperature negatively impact the symbiosis of corals and zooxanthellae, reducing the photosynthetic performance, deteriorating nutrient transfer between host and symbiont, which results in coral bleaching and threatening the survival of tropical coral communities (Coles and Jokiel, 1978; Fitt *et al.*, 2001; Humphrey *et al.*, 2008; Kuanui *et al.*, 2015). Additionally, the combined effects of hypoosmotic and elevated thermal stress impair the fertilization (Humphrey *et al.*, 2008), settlement (Tam and Ang Jr, 2008), and embryonic development, resulting in an 80 % decline in the reproduction success of the tropical Scleractinia *Platygyra acuta* (Chui *et al.*, 2015).

Therefore, knowledge of the impact of altered temperature and salinity in marine habitats on physiological performance, e.g., metabolic activity and calcification rates, and reproduction is essential for understanding the threats corals currently face. It is important to determine species-specific thresholds for temperature and salinity of species important for the ecosystem function and are at risk and support relevant stakeholders in developing effective conservation strategies.

## 1.5 The cosmopolitan cold-water coral *Desmophyllum dianthus*

The scleractinian CWC *Desmophyllum dianthus* (Esper, 1794), is a solitary, ahermatypic CWC species that occurs mainly in the deep sea. It has a cosmopolitan distribution and a wide bathymetric range from 8 to 4,000 m depth (Fig. 1; Risk *et al.*, 2002; Försterra and Häussermann, 2003; Försterra *et al.*, 2005). Its habitat, which is predominantly in the bathyal zone, is characterized by rugged topography, so that populations of *D. dianthus* are mainly restricted to the margins of continental shelves, offshore submarine banks, canyons, and fjords, built by hard substrates (Freiwald *et al.*, 2004). Many populations are located in the deep sea of the northern and western Atlantic (Sorauf and Jell, 1977; Cogswell *et al.*, 2009) and the Pacific (Cairns, 1994). This CWC species is also very abundant in temperate regions of the central and northwestern Mediterranean Sea, in a depth range from 250 m to 1,200 m (Taviani *et al.*, 2005, 2017; Freiwald *et al.*, 2009; Orejas *et al.*, 2009; Taviani *et al.*, 2017), where it is exposed to a temperature range of 11 °C to 14 °C (Palanques *et al.*, 2006) and a salinity range of 38.1 – 38.9 [PSU-scale] (Millero *et al.*, 1979; Klein *et al.*, 1999; Schneider *et al.*, 2007). Mediterranean *D. dianthus* species are known to form complex three-dimensional biogenic frameworks with other scleractinian CWCs such as *D. pertusum* and *Madrepora oculata*, providing habitats for various marine species (Freiwald *et al.*, 2009; Roberts *et al.*, 2009; Angeletti *et al.* 2014; Taviani *et al.*, 2017; Chimienti *et al.* 2018).

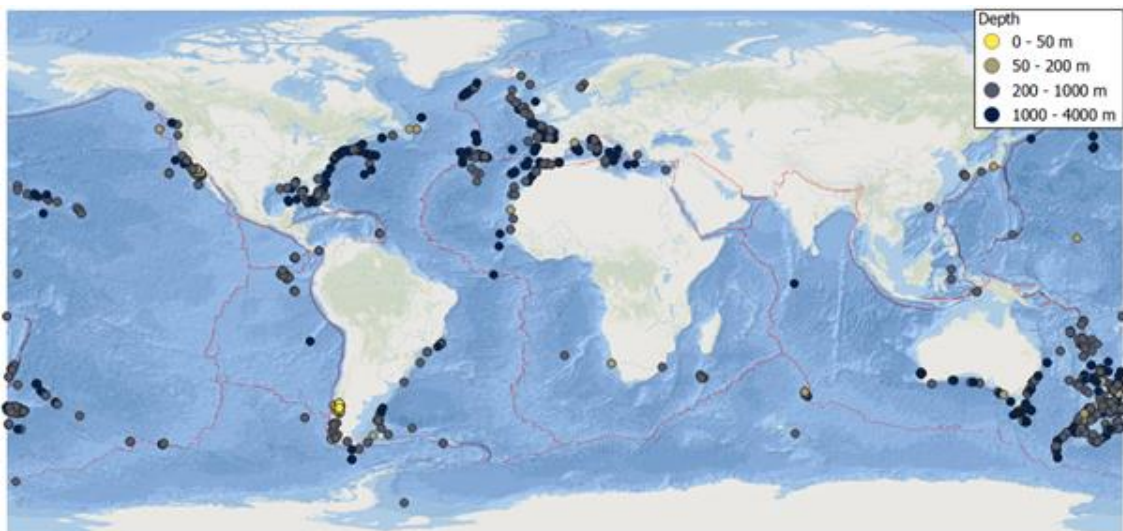


Figure 1: Global distribution of *Desmophyllum dianthus*. The bathymetric location of populations is divided into four classes: euphotic zone: 0 - 50 (surface layer) and 50 - 200 m, dysphotic zone: 200 - 1000 m, and aphotic zone: >1000 m) near continental shelves and submarine canyons, fjords, trenches, and ridges characterized by steep slopes as they occur at the boundaries of tectonic plates (red lines). Map derived from QGIS (version 3.14.16π); Basemap: ESRI Ocean/Tectonic Plates; data layer: OBIS(UN Environment Programme World Conservation Monitoring Centre).

Few dense populations of *D. dianthus* were recorded in temperate shallow waters, e.g. on the coast of New Zealand (Grange *et al.*, 1981; Cairns, 1995; McCulloch *et al.*, 2005) and in the stratified Chilean Fjords (Risk *et al.*, 2002; Försterra and Häussermann, 2001, 2003; Häussermann and Försterra, 2007). Especially in northern Chilean Fjords, *D. dianthus* constitutes a dominant species in benthic communities (Freiwald *et al.*, 2004; Försterra *et al.*, 2005). Individuals are found sporadically at 12 m and in aggregations of more than 1,500 species m<sup>-2</sup> below 18 m (Försterra and Häussermann, 2003; Jantzen *et al.*, 2013a). Due to intraspecific competition for a favorable exposure of polyps to food-bearing currents, individuals in dense aggregations and pseudo-colonies, as a result of secondary recruitment (Försterra and Häussermann, 2003), form large and tubular aragonite skeletons with thin walls, in contrast to isolated organisms characterized by their shortness and trumpet-shaped corallites (Cairns *et al.*, 2005). In general, specimens among one population and specimens of different populations are characterized by morphological variation of the polyp and aragonite exoskeletons (Addamo *et al.*, 2015; Cairns, 1994).

### 1.6 The Chilean population of *D. dianthus*

The coral constitutes one of the best studied Scleractinia in the Pacific (see references in this subchapter). It dominates the benthic marine habitat on hard substrates in Chilean fjords (Försterra *et al.*, 2005; Försterra and Häussermann, 2005).

Most studies took place in Comau Fjord, due to its easy accessibility and environmental conditions, which offer the possibility to study, for example, the effect of low pH on species building aragonite skeletons (Jantzen *et al.*, 2013a; Movilla *et al.*, 2014; Carreiro-Silva *et al.*, 2014, Försterra *et al.*, 2016). Comau Fjord in Chilean Patagonia with its almost vertical basaltic walls is connected to the Gulf of Ancud via the Chago Channel and reaches a maximum depth of 487 m, while the minimum depth of 50 m is found at its head. The fjord has a maximum length of 45 km from its mouth near Liguapi Island to Lepto and a maximum width of 8.5 km (Häussermann *et al.*, 2012).

The upper water layer is subject to strong seasonal fluctuations in temperature from 8 to 13.5 °C and salinity ranging from 28.5 to 34 [PSU-scale] (Försterra *et al.*, 2005; Beck *et al.*, 2022). Shallow-dwelling *D. dianthus* specimens are exposed to strong environmental fluctuations, caused by tides with a maximum height of up to 7.42 m (Schwabe *et al.*, 2006), seasonal changes in plankton abundance (Garcia-Herrera *et al.*, 2022), and strong fluctuations in nutrients (Castro *et al.*, 2011), aragonite saturation ( $\Omega_{\text{arag}}$ ) (Beck *et al.*, 2022), oxygen content, salinity and

temperature (Palma and Silva, 2004; Silva, 2008; Försterra *et al.*, 2005; Fillinger and Richter, 2013; Jantzen *et al.*, 2013a). The upper water layer is characterized by large temperature fluctuations mainly driven by seasons, and reduced salinity generated by heavy rainfall and rural freshwater input (Silva, 2008; Häussermann *et al.*, 2012; Fillinger and Richter, 2013), while hyperosmotic conditions occur due to increased evaporation, low water movement and reduced freshwater input (Sheppard *et al.*, 2009). While the water layers below the pycnocline exhibit more stable environmental conditions, characterized by an average temperature of 11°C and salinity of 31 [PSU-scale] (Fillinger and Richter, 2013; Jantzen *et al.*, 2013; Beck *et al.*, 2022).

## 2 Knowledge gaps and aim of the study

In general, the effect of hyperosmotic conditions compared to hypoosmotic conditions on scleractinian corals is very limited. Only Cowlin *et al.* (2012) address the effects of elevated salinity on the metabolism of the tropical coral *Acropora aspera*. No study has been conducted to assess the vulnerability of CWCs to increased salinity. To simultaneously improve the understanding of *D. dianthus* population dynamics, this study tests the potential effects of elevated salinity and temperature to which populations are exposed in the deep Mediterranean Sea on specimens of Chilean populations thriving under lower average annual salinity and temperature in the fjord.

The aim of this study was to investigate whether the abundance and cosmopolitan occurrence of *D. dianthus* are driven due to phenotypic plasticity, which describes the acclimation potential that enables efficient physiological activities without evolutionary adaptation of an organism. For this purpose, specimens of the Chilean population are exposed to altered salinity and temperature conditions. To investigate the single and synergistic effects of these two parameters, uni- and multifactorial treatments were performed in which the animals were subjected to the mean deep-sea Mediterranean temperature of 12 °C, and in a second treatment to the increased temperature of 12 °C and the mean deep-sea Mediterranean salinity of 38. I examined changes in behavior, respiration, and growth of *D. dianthus* specimens during the phase where I gradually changed the environmental parameters and under the final environmental conditions.

The behavioral adaptability of the coral specimens to the altered environmental factors is assessed by observing the contraction and elongation of the tentacles, as the rate of extension regulates nutritional supply and therefore provides the basis for any physiological performance e.g. calcification (Naumann *et al.*, 2011; Fähse, 2021). Since respiration is essential for

intracellular energy production to maintain metabolic activity and osmoregulatory processes, a change in respiration rate represents an important indicator of altered bioenergetic costs in organisms (Gilles, 1973; Goolish and Burton, 1989; Willmer *et al.*, 2005). Using two metodological approaches, measure of the polyp calyx and buoyant weighing, growth changes are determined based on changes in the calyx area and mass variation under different experimental conditions.

The main objective of this study was to determine the acclimation capability of Chilean *D. dianthus* specimens to the temperature and salinity to which this species is exposed in the Mediterranean Sea. The experiment lasted three months. To this end, the study addressed the following hypotheses:

Hypothesis 1: The polyp extension of *D. dianthus* specimens is influenced by increased temperature and salinity.

Null hypothesis 1: The polyp extension of *D. dianthus* specimens is not influenced by increased temperature and salinity.

Hypothesis 2: The respiration rate of *D. dianthus* increases with elevated temperature or salinity.

Null hypothesis 2: The respiration rate of *D. dianthus* is not increased with elevated temperature or salinity.

Hypothesis 3: The growth of *D. dianthus* is impacted by increased temperature and salinity.

Null hypothesis 3: The growth of *D. dianthus* is not impacted by increased temperature and salinity.

## 3 Material and methods

### 3.1 Sampling of *D. dianthus* from Chilean Comau Fjord

Specimens of the scleractinian CWC *D. dianthus* were chiseled from the substrate by scientific SCUBA divers in Chilean Comau Fjord (42° 23.244'S; 72° 27.669'W) at a depth of 27 m and at Caleta Soledad (41° 40.373'S; 72° 39.396'W) at 32 m in April and May 2021. Thereafter the corals were transported to the aquaria facilities at the Alfred Wegener Institute (AWI, Bremerhaven, Germany) (Fig. 2).



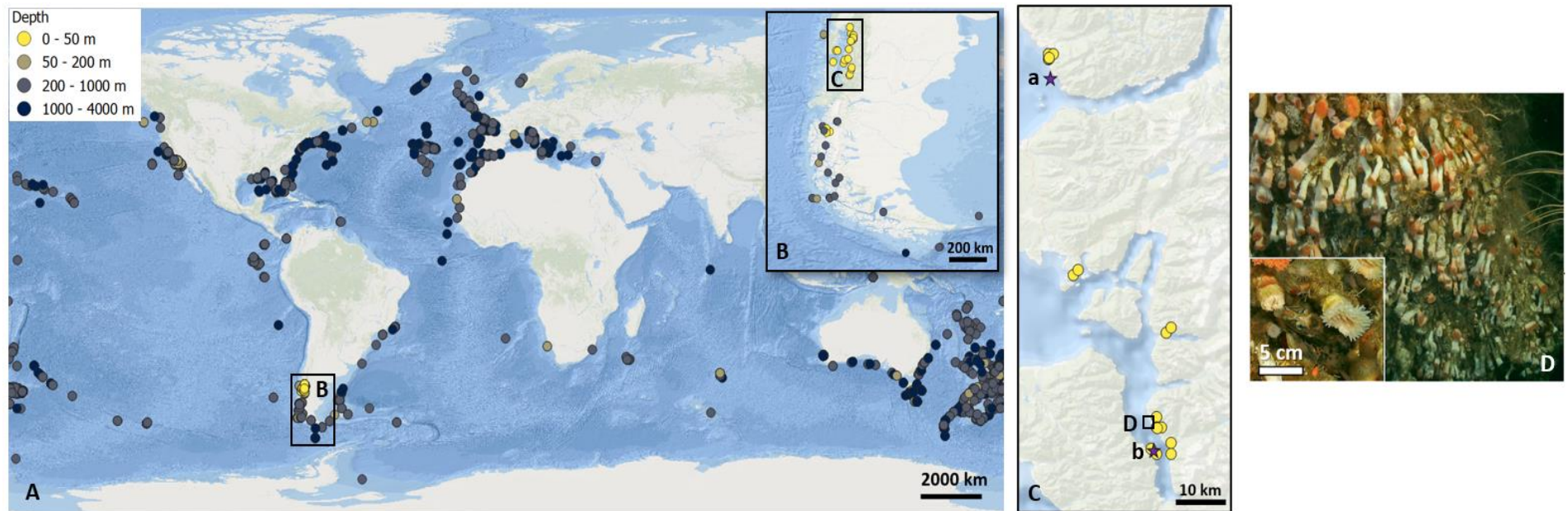


Figure 2: **A**) Global distribution of *Desmophyllum dianthus* populations in different bathymetrical zones (OBIS, UN Environment Program World Conservation Monitoring Centre). Populations in shallow depth found in **B**) Patagonian Fjord System where laboratory specimens were sampled at **c**) Caleta Soledad (**a**) and Comau Fjord (**b**) **D**) from dense aggregation **D**) (Försterra et al. 2016).

In the aquarium facility, the corals were kept in the dark at 11 °C and a salinity of 31 [PSU-scale], which corresponds to *in situ* conditions (Fillinger and Richter, 2013), for seven months until the specimens were transferred into the experimental set-up. Corals were fed two times a week with *Artemia franciscana* and once with juvenile krill, additional 50 % of the artificial seawater was exchanged once a week.

### 3.2 Preparation of *D. dianthus* specimens

Prior to the start of the acclimation period and before conducting the experiment, all corals were detached from any remaining hard substrate and individual polyps of pseudo-colonies were separated. For this purpose, a Speed Rotary Tool with cutting disc was used (Dremel 8200, USA) to separate the corals from the substrates above the water line, while the polyps were kept under water to diminish stress. Afterwards, each coral was cleaned of fouling with tweezers and a toothbrush. All animals were transferred back to their aquaria facility. After measuring the initial mass via the buoyant weight technique (Jokiel et al., 1978), each coral was fixed with coral glue (easy glue, Preis Aquaristik, Germany) on plastic screws, labeled individually with bee number plates (Abelo, United Kingdom) and placed back into the aquarium facility.

### 3.3 Experimental design

The experimental setup was allocated in a thermostatically controlled room at 8 °C in complete darkness in the AWI aquarium facilities from 17<sup>th</sup> of January to 18<sup>th</sup> of May 2022.

A total of 21 *D. dianthus* specimens were evenly distributed based on their size and mass into three equal groups: 1) the control group (C; N = 7) was maintained under the natural environmental conditions at the sample site of Comau Fjord (Chile) (Temperature: 11 °C, Salinity: 31 [PSU-scale]); 2) a second group (Treatment 1, T1; N = 7) was maintained at deep-sea Mediterranean temperature of 12 °C and Chilean salinity of 31 [PSU-scale], and 3) the third group (Treatment 2, T2; N = 7), was maintained at 12 °C and 38 [PSU-scale] corresponding to the average deep-sea Mediterranean salinity and temperature. For true replication, each coral was placed in a glass bottle (500 mL-Schott wide-necked jar, Duran, Germany). Constant water supply was maintained with filtered and UV-treated artificial sea water by gravity from a reservoir tank via one separate plastic hose with a flow rate of 0.2 L min<sup>-1</sup>. The bottles were placed in a water bath with submersible pumps to maintain a constant temperature. The temperature was controlled by temperature switches (TS 125, H-Tronic, Germany) and a titanium heater (SCHEGO, Germany) with a step size of 0.1 °C, which was switched on if

temperature decreased to 10.9 °C. The rim of the glass bottles was always above the water level of the water bath, so that excess water could run off (Fig. 3).



Figure 3: **A)** Experimental setup. The flow of water by gravity from the water reservoir tanks ① through separated water inlet hoses ② guarantees continuous flow into seven 500 mL Schott glass bottles, which are placed in a water bath ③. The outflow of the water bath takes place into the catch basin ④. After filtering and treatment with UV light, the water was pumped back into the water reservoir tanks. **B)** Close-up of one experimental coral placed in the middle of a glass bottle (2.5 x zoom).

### 3.3.1 Acclimation to experimental treatments

The control group (C) was maintained throughout the acclimation and the experimental phase under constant conditions (here named 'experimental phase') at the average Chilean salinity of 31 and temperature of 11 °C. The specimens of T1 and T2 were subjected to a stepwise acclimation process to the targeted experimental conditions (Fig. 4).

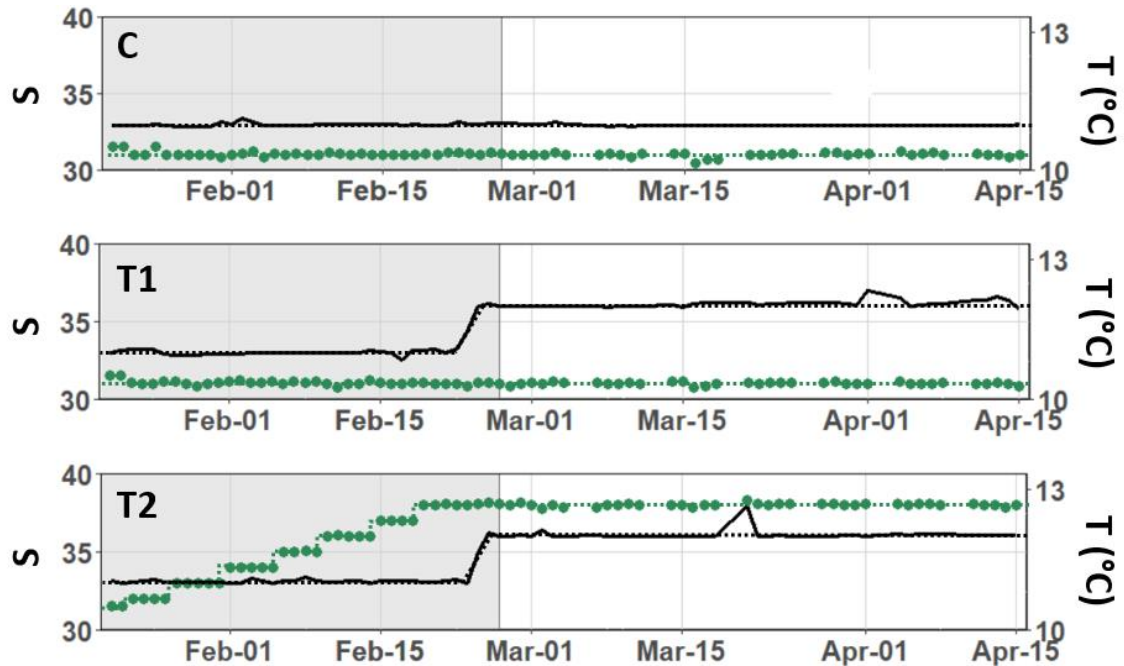


Figure 4: **Timeline of experimental conditions.** Timeline of salinity (predicted: green dotted line; measured: green dots) and temperature (predicted: black dotted line; measured: black solid line) in control (C), treatment 1 (T1) and treatment 2 (T2) during acclimation (grey background) and experimental phase (white background). **Upper plot:** the salinity and temperature of C remained during the whole acclimation and experimental phase at an average of 31 and 11 °C. **Middle plot:** the salinity was retained at 31 while temperature was elevated to 12 °C in T1 during acclimation and maintained in experimental phase. **Lower plot:** the salinity of T2 was increased stepwise from 31 to 38 and the temperature increased to 12 °C during acclimation and maintained during the experimental phase.

To test the single effect of elevated temperature, Treatment 1 (T1) was maintained at average Chilean salinity of 31 while the temperature was increased from the average Chilean temperature of 11 °C over two days to the deep-sea Mediterranean temperature of 12 °C at the end of the salinity acclimation. The environmental condition of T2 was set in acclimation to average deep-sea Mediterranean temperature and salinity; while the temperature was elevated parallel to the increase performed in T1, salinity was increased one unit every four days with reef salt (Premium Reef Salt, Dupla Marin, Germany) during the acclimation.

### 3.3.2 Feeding and maintenance of corals

Corals were fed in the morning, as the best feeding time is between 06:00 and 12:00 due to high protein and protease activity, as determined for *D. dianthus* by Ding *et al.* (2022).

The corals were fed three times a week with two different prey items: *Artemia franciscana* nauplii (REBIE, Germany) and thawed juvenile krill *Euphausia pacifica* (Zierfischfutterhandel Norbert Erdmann e.K., Germany). In total 2.5 g *Artemia franciscana* eggs were incubated for 48 h at 25 °C in a funnel with 1 L artificial seawater and continuous air supply. After hatching, larvae and eggs were separated using a 100 µm sieve and concentrated in 300 mL artificial seawater. Then, 10 ml of the *A. franciscana* suspension (corresponding to a concentration of 83.3 nauplii L<sup>-1</sup>) was added to each glass bottle containing one coral using a 100 mL-syringe. The water supply through the inlet hose was interrupted to maintain all *A. franciscana* specimens for 4 h in the glass bottle.

In addition, each coral was fed with a *E. pacifica* specimen once a week with tweezers. The combination of two different food items guarantees the adequate nutrition for this scleractinian species (Gori *et al.*, 2015). To remove food debris from C, T1, and T2, 100 µm-meshes were placed over each catch basin inflow tube, and the water bath and bottles were cleaned weekly. During the latter, 100 L of aquarium water (50 % of the total water volume) was replaced with 80 L new artificial water and 20 L nutrient rich water from the culturing aquarium system.

### 3.3.3 Monitoring of environmental parameters

Physical and chemical parameters were measured throughout the experiment. Temperature was recorded through the experiment every 15 min by two HOBO Data Loggers (Hoboware, USA) per treatment. While one of the loggers recorded temperature continuously until the end of the experiment, the second logger was used to check the degree of stability and/or possible fluctuations of the temperature in each tank every two weeks using the HOBO Data Loggers & Devices software (Version 3.7.8, onset HOBOWare, USA). Salinity (Salinometer Cond 3110, WTW, Germany), pH (ph3310, WTW, Germany) and dissolved oxygen concentration (DO-instrument, ProODO dissolved oxygen instrument, YSI Incorporated, USA) were manually measured in each aquarium five times a week. Seawater density was calculated ( $\rho_{SW}$ , kg m<sup>-3</sup>) according to the water density formula (Massel, 2015) and transformed to sigma-theta ( $\sigma_\theta$ ) by using equation 1.

$$\sigma_\theta = \rho_{SW} - 1000 \text{ kg m}^{-3} \quad (\text{Eq. 1})$$

Nutrient concentrations were measured weekly with a photometer (NOVA 60 SA, Spectroquant Merck KGaA, Germany). For this purpose, 150 mL-water samples were taken from one of the water reservoir tanks of C, T1, and T2. A subsample of 50 mL was filtered using a 60 ml-syringe and glass microfiber filters (GF/FWhatman, UK) before measuring dissolved nutrients. Samples were prepared for photometric measurements of nitrate, nitrite, ammonium ions, dissolved ammonia and phosphate (all test from Merck KGaA, Germany). Measurements were carried out in 10 and 50 mm-glass cuvettes against a blank sample consisting of ultrapure Milli-Q water (Sartorius arium pro, Germany). Furthermore, rapid test kits (Nitrate Test Algenkontrolle; Nitrite Test Filterkontrolle; Ammonium/Ammoniak Test Filterkontrolle, Phosphate Test Algenkontrolle, JBL GmbH & CO KG, Germany) were used to control photometric determined nutrient concentrations.

The latter were converted from  $\text{mg L}^{-1}$  to  $\mu\text{mol kg}^{-1}$  SW using Equation 2 and considering the molar mass from each nutrient and the water density.

$$c_{cal} = \frac{c_p \cdot 1000}{\frac{MM}{\rho_S}} \quad (\text{Eq. 2})$$

$c_{cal}$  = calculated concentration ( $\mu\text{mol kg}^{-1}$ )

$c_p$  = photometrical concentration ( $\text{mg L}^{-1}$ )

$MM$  = molar mass ( $\mu\text{g } \mu\text{mol}^{-1}$ )

$\rho_S$  = sea water density (Massel, 2015)

Total alkalinity (TA) was determined weekly by potentiometric titration. For this purpose, 250 mL water were collected from the reservoir tank of C, T1, and T2. All water samples were filtered using glass microfiber filters (GF/F, Whatman) and transferred into 50 mL-glasses (Duran, Schott, Germany), placed in a sample changer for automatic titration (SI Analytics TW alpha plus, Germany) together with two replicates of our in-house North Sea seawater standard. The measurement was controlled by the automatic titrator system (TitroLine alpha plus, Germany) with TitrSoft (Xylem Analytics, Germany). The obtained TA ( $\text{mol L}^{-1}$ ) data were converted to  $\mu\text{mol kg}^{-1}$  (Equation 3), considering salinity and water density, and normalized to the mean alkalinity value of the North Sea seawater standard. TA ( $\mu\text{mol kg}^{-1}$ ), temperature and pH values were used to calculate the aragonite saturation and bicarbonate concentration, essential for the formation of aragonite skeletons using CO2SYS (Pierrot *et al.*, 2006).

$$c_{TA\_cal} = \frac{c_{TA}}{\rho_S} \quad (\text{Eq. 3})$$

$C_{TA,cal}$  = calculated TA concentration ( $\mu\text{mol kg}^{-1}$ )

$C_{TA}$  = TA concentration ( $\mu\text{mol L}^{-1}$ )

$\rho_S$  = Sea water density (Massel, 2015)

### 3.4 Response variables

To study the single effect of elevated temperature and the interactive effect of hypersalinity and elevated temperature, four different response variables were considered: (1) polyp extension, (2) respiration and (3) growth related to skeletal mass and (4) calyx area variation. The polyp behavior was monitored by visual observations of the polyp extension in the morning and evening throughout the acclimation and experimental phase. The mass-specific respiration rate was determined at the end of the acclimation and experimental phase to determine metabolic reaction to short-term (3 days) and long-term (50 days) maintenance under hypersaline and hyperthermal conditions. Additionally, growth was determined throughout the acclimation and experimental phase, by determining skeletal corals' mass and calyx area at the beginning and end of the acclimation and at the end of the experimental phase.

#### 3.4.1 Polyp extension

The behavior of polyps during stress conditions, whose adaptability can be assessed by stretching and contracting polyps and tentacles, was analyzed based on the diurnal polyp extension rates (Ding *et al.*, 2022). The polyp activity was tested in response to the single effect of increased temperature and interactive effect of increased temperature and elevated salinity comparing two periods of the day. The polyp activity was documented in the morning (09:00 – 11:00) and evening (17:00 – 19:00), when any feeding and/or mechanical stress due to water changes and coral handling were absent for eight hours before the observations.

Since activities occurred during the day and no handling was conducted at night, the sample size of the morning (N= 44) observations was 4.4 times larger than the data set of the evening (N= 10) observations. Following a slightly modified approach of Torrents *et al.* (2009) and Prevati *et al.* (2010), polyp extension was categorized into three different modes of activity: retracted (0 % extension), semi-expanded (50 % extension), and fully expanded polyps (100 % extension) (Fig. 5). The mean polyp extension ( $\underline{PE}$ ) was then calculated by equation 4 (Faehse 2021):

$$\underline{PE} = \frac{\sum_{i=1}^n PE}{n} \quad (\text{Eq: 4})$$



Figure 5: Categories of the degree of polyp expansion of *Desmophyllum dianthus*, from left to right: 0 % expansion, 50 % expansion and 100 % expansion.

The mean polyp expansion for C, T1, and T2 during morning and evening was calculated and analyzed regarding significant differences applying statistical test (described in chapter 3.5).

### 3.4.2 Respiration rates

Respiration rates were used to document changes in metabolic processes caused by external stress. To study the short- and long-term impact of hyperosmotic and/or elevated temperature stress, respiration rates were measured after the corals were exposed to the treatments for 3 and 50 days.

To measure the baseline respiration rate of *D. dianthus*, the corals were starved for 24 h prior to the measurements to eliminate any influence of metabolic activity due to digestion (Dodds *et al.*, 2007).

Twelve incubation chambers (100 mL Duran bottles; Schott, Duran, Germany) were equipped with oxygen sensor spots (OXSP4, Pyroscience, Germany) using E43 silicone rubber (RTV-1, Wacker Silicones Elastosil, Germany). The tips of 5 mL plastic syringes were used as adapters for the sensor spots and fixed outside the labeled incubation chambers with tape. A M8 nut was glued into the plastic lid of each chamber to fix tested corals.

The respiration measurements took place in a constant temperature room (8 °C) in a water bath. The temperature of the water bath was adjusted to treatment conditions and controlled with an aquarium thermostat (T-Computer, AquaMedic, Germany), which controlled a titanium heater. A submersible flow pump (NewJet Wave Nano, France) ensured uniform temperature distribution in the water bath. The incubation chambers were placed on a submersible, multi-magnetic stirrer plate (Variomag H+P Telesystem, Germany) (Fig. 6).

Each incubation chamber was connected via optic fibers (SPFIIB-Bare-CL2, PyroScience, Germany) to fiber optic multi-analyte meters (FireSting O<sub>2</sub> / pro, PyroScience, Germany), while a temperature probe (PT100 TSub21, PyroScience Germany) monitored the temperature. As the hardware equipment is not waterproof, all oxygen meters were individually housed in waterproof boxes (DRiBOX, United Kingdom). All three oxygen meters were controlled by a computer software. While FireSting pros are operated by Pyro workbench (Version V1.32.1966, PyroScience, Germany), FireSting O<sub>2</sub> is controlled via Pyro Oxygen Logger (V.3.213 2013, PyroScience, Germany).

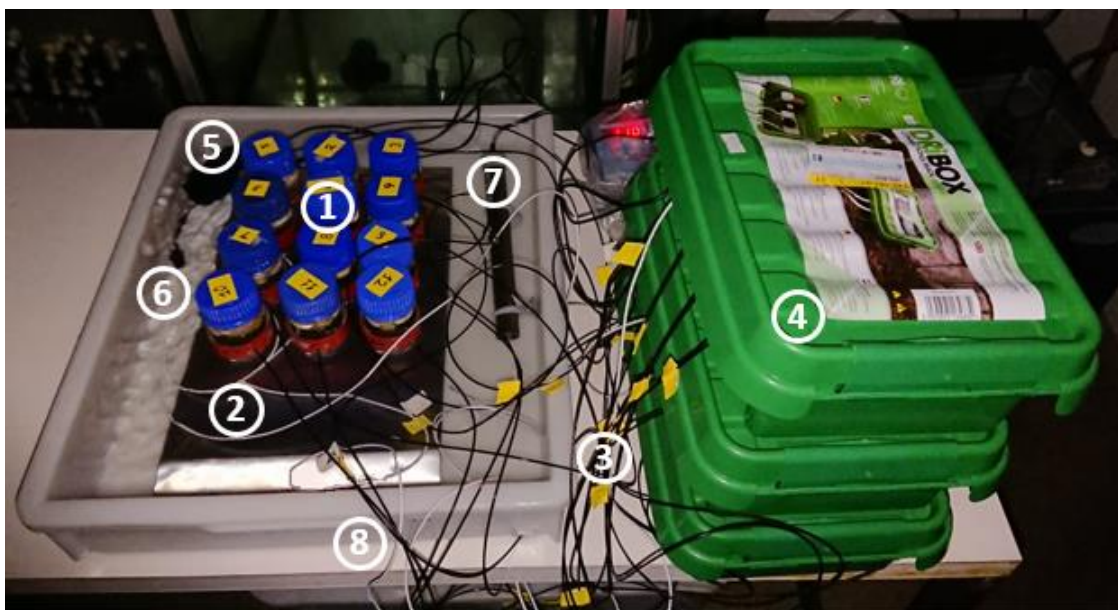


Figure 6: Experimental setup for respiration measurements. Twelve incubation chambers (1) were placed on a multi-magnetic stirrer (2) and equipped with internal oxygen sensors connected by optical fibers (3) to three oxygen meters located in waterproof boxes (4). The water in the water bath was kept circulating by a pump (5). The temperature was controlled by a temperature sensor (6), steered by a titanium heater (7) and measured by three white sensors (8) connected to the oxygen meters.

Prior to the measurements, each sensor spot was calibrated with oxygen-free tap water and 100 % oxygen-saturated saltwater at the treatment temperature. For this purpose, 1 g L<sup>-1</sup> sodium dithionite was dissolved in freshwater, while the saltwater was aerated for 30 min with compressed air using an air stone. Both calibration solutions were checked for oxygen concentration using the DO-Instrument (ProODO, YSI Incorporated, USA).

Before the corals were introduced in the experimental chambers, epifauna was removed from the skeleton and the screw with a toothbrush (Sokol, 2012) and fixed in the lid of the incubation chamber. To prevent erroneous measurements, air bubbles were removed with a brush before closing the chamber, and the oxygen concentration in the water was homogenized throughout

the measurement with a glass-encased magnetic stirrer). The oxygen concentration in the incubation chambers was measured during six hours in the dark by luminescence-based oxygen measurement to ensure a visible analyzable oxygen consumption without damaging the corals by hypoxia (Dodds *et al.*, 2017). Simultaneously, the oxygen saturation in four incubation chambers filled with filtered seawater only was measured to determine the background respiration by microorganisms.

### 3.4.2.2 Determination of Ash-Free-Dry-Mass (AFDM)

To relate the measured respiration rate to the oxygen-consuming biomass only, neglecting the mass of the aragonite skeleton, the organic mass of the polyp was determined using ash-free dry mass (AFDM).

For this purpose, corals of C, T1, and T2 were shock-frozen in liquid nitrogen at the end of the experiment and stored in a -80 °C freezer. All frozen *D. dianthus* specimens were crushed with a hammer to ensure complete drying of the polyp. The corals were placed into pre-combusted aluminum trays and dried in an oven at 60°C for 24 h. Thereafter, the dry mass ( $M_{D+pan}$  [g]) was determined using a high-resolution analytical balance (CPA225D-0CE, Sartorius). Further, organic carbon was removed by burning the coral samples in the aluminum trays in a muffle furnace at 500°C for 24 h and the ashed mass was measured. By using the dry ( $M_{D+pan}$ , g) and ash mass ( $M_{A+pan}$ , g) and the weight of the pan, the AFDM (mg) was determined according to equation 5.

$$AFDM = \frac{M_{D+pan} - M_{A+pan}}{1000} \quad (\text{Eq: 5})$$

### 3.4.2.3 Computation of mass-specific respiration rates

Raw data in dphi units were converted into mg O<sub>2</sub> L<sup>-1</sup>, by taking into account the calibration settings, pressure, salinity, and temperature using the Oxygen Calculation Tool (PyroScience, Germany). Using the rMR package (rMR\_1.1.0, Moulton, 2018), metabolic rates (MR) of three 2-hour intervals were calculated to control for slope constancy over time ( $R^2 \geq 0.95$ ). The incubation volume in L ( $V_{inc}$ ) was used to adjust the mean metabolic rates. The latter were calculated by subtracting the background metabolic rate ( $MR_{BG}$ ) to obtain the oxygen consumed per coral. The rates obtained were normalized for the AFDM and multiplied by 24 to obtain individual metabolic rates per day ( $MR_{day}$ ) (equation 6).

$$MR_{day} = \frac{\sum_{i=1}^n MR}{n} \frac{V_{inc} - MR_{BG}}{AFDM} * 24 \quad (\text{Eq: 6})$$

### 3.4.3 Growth

At the beginning and after the acclimation and experimental phase, the buoyant mass of each individual was measured using the buoyant weight technique (Fig. 8). With this method, the dry mass of the aragonite skeleton is determined from the mass in seawater based on Archimedes' principle, considering the density of the skeleton and the seawater (Jokiel *et al.*, 1978, Davies, 1989).

For this purpose, an analytical balance with a resolution of 0.01 mg (CPA225D-0CE, Sartorius) and an underfloor weighing device was used. A connected metal weighing basket was completely submerged in a 10 L aquarium containing seawater at a temperature of 11 °C ± 0.5 °C or 12 °C ± 0.5 °C, respectively. After filling the aquarium, the salinity was measured, and the water temperature was continuously monitored with a digital thermometer. Cool packs were used to keep the temperature approximately the same, and if the temperature rose more than 0.5 °C, some water was replaced by colder water.

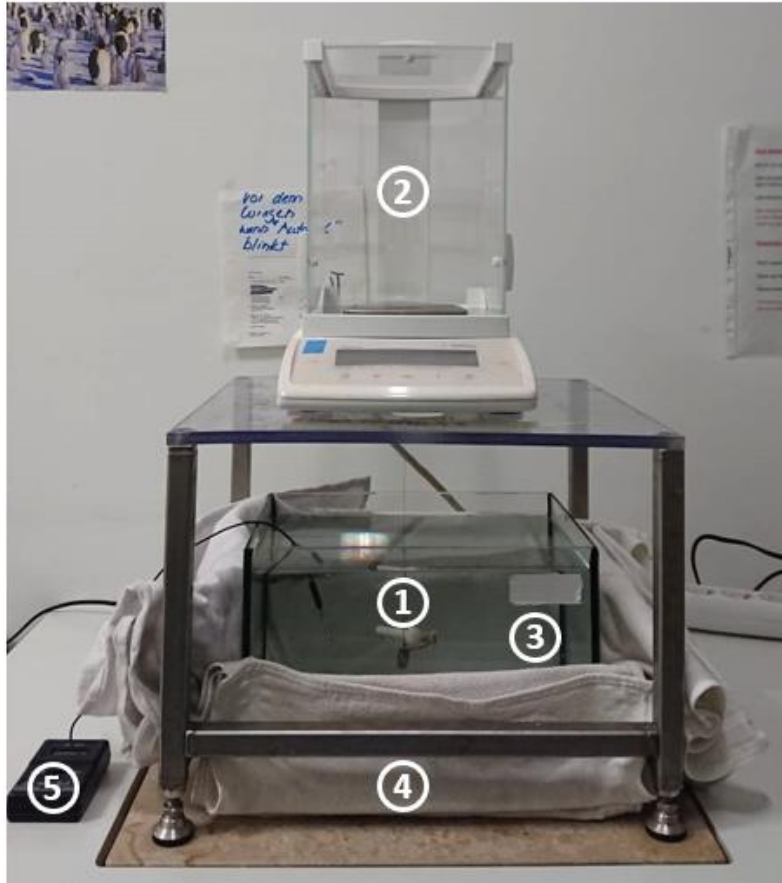


Figure 8: The buoyant mass of corals ① was measured with a high-resolution balance ② placed above a water bath ③. The temperature of the water in the aquarium was controlled by four cool packs ④ and continuously monitored with a thermometer ⑤.

Air bubbles that can influence the accuracy of the mass measurements were carefully removed with a brush. Due to the high sensibility of the balance, the mass readings were considered valid if they remained stable for 15 seconds. A series of three measurements were performed and the mean buoyant mass was determined. To obtain the coral mass, the mass of the plastic screw was subtracted from the total mass. Salinity and temperature were used to calculate seawater density ( $\rho_{SW}$ ) according to the formula of Massel (2015). The skeletal dry mass at a given time ( $M_{dtn}$ ) of each coral was calculated according to equation 7 (Jokiel *et al.*, 1978), considering the density of aragonite ( $\rho_{arag} = 2.835 \text{ g cm}^{-3}$ ; Naumann *et al.*, 2013), of which the skeleton of *D. dianthus* is composed of.

$$M_{dtn} = \frac{M_{bw}}{1 - \frac{\rho_{SW}}{\rho_{arag}}} \quad (\text{Eq: 7})$$

The growth rate, expressed as percentage growth per day ( $G_t(M)[\% \text{ day}^{-1}]$ ) during the five-week acclimation and experimental phase of seven weeks, was determined using equation 8, respectively (Jokiel *et al.*, 1978; Orejas *et al.* 2011a, b).

$$G_t(M) = \frac{M_{t+1} - M_t}{M_t(T_{t+1} - T_t)} * 100 \quad (\text{Eq: 8})$$

$G_t(M)$  = skeletal dry mass growth rate

$M_t/M_{t+1}$  = skeletal dry mass at point in time

$T_t/T_{t+1}$  = point in time (numeric) of measurement

#### 3.4.4 Calyx area variation

To determine morphological changes in growth related to the different environmental conditions during ramping and experimental phase, the variation of the calyx area was determined by means of digital photographs (Sony Cyber-shot RX10 IV, Japan), using external lightning (LED Flat 200 Walimex pro, Germany), at three time points: beginning and end of acclimation and final end of acclimation. Each coral (N= 7 per treatment) was placed in a customized holder at a fixed distance from the camera lens in a horizontal position; a scale was attached to the inner wall of the aquarium near the coral. The image was artificially exposed with an external LED light (LED Flat 200 Walimex pro, Germany).

Subsequently, the calyx area was determined using the Java-based image processing program ImageJ (1.53k, National Institutes of Health, USA). In the beginning of the area acquisition, the number of pixels included in a polygon was computed and transformed to  $\text{cm}^2$  based on the photographed scales. In the next step, the number of pixels comprised in the calyx surface in the image was determined by a manually defined polygon (Fig. 7).

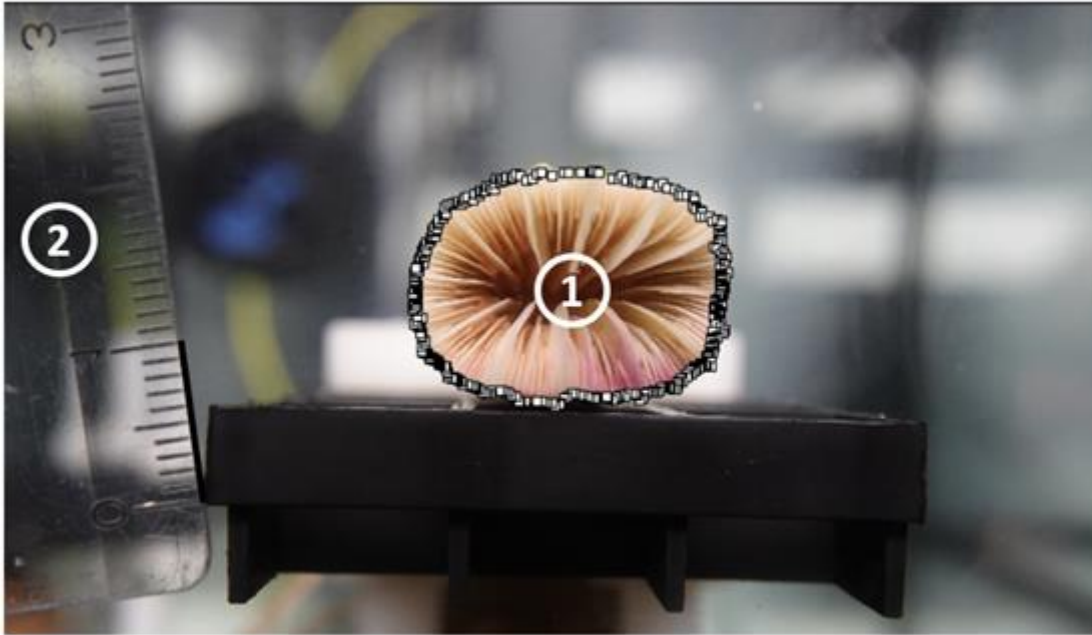


Figure 7: Processed image for determining the calyx area. Using image processing software (ImageJ), the area of a polygon whose vertices are defined by white rectangles ① is calculated using the scale of a ruler ②.

After the corals' calyx surface areas of C, T1, and T2 were computed, the individual growth rate [% d<sup>-1</sup>] of the acclimation and experimental phase was calculated, applying equation 9.

$$G_t(A) = \frac{A_{t+1} - A_t}{A_t(T_{t+1} - T_t)} * 100 \quad (\text{Eq: 9})$$

$G_t(A)$  = calyx area growth rate

$A_t/A_{t+1}$  = calyx area measure per time interval

$T_t/T_{t+1}$  = time of measurement

### 3.5 Statistical analysis

All data were analyzed graphically and statistically in R, defining  $\alpha = 0.05$  for Type I error. Values were expressed as mean  $\pm$  standard deviation (SD). The normal distribution and homoscedasticity were examined using the Shapiro-Wilks and Bartlett test, performed with the package 'stats' (version 3.6.2; R core team, 2021), while the datasets were checked regarding outliers with Dixon Q test of the package 'outlier' (version 0.15; Komsta 2022). If the assumption for parametric statistic tests was fulfilled, a univariate one-way ANOVA and, if significant, subsequently posthoc Tukey Honestly Significant Differences (HSD) of the R package 'stats' (version 3.6.2; R core team, 2021) was conducted. Nonparametric tests were performed, if outliers exist, unbalanced datasets were compared, normality or homoscedasticity could not be proven. To compare more than two datasets, a Kruskal-Wallis rank sum test, and if significant, Wilcoxon tests were performed to identify relevant differences between the control and treatments using the package 'stats' (version 3.6.2; R core team, 2021). To identify relationships among water parameters and impacts on response variables Spearman correlations were determined with the package 'stats' (version 3.6.2; R core team, 2021).

## 4 Results

In the following section, the physical and chemical parameters, temperature (T), salinity (S), seawater density ( $\sigma_\theta$ ), oxygen concentration ( $O_2$ ), pH, nutrient concentration of nitrate ( $NO_3^-$ ), nitrite ( $NO_2^-$ ), ammonium ( $NH_4^+$ ), phosphate ( $PO_4^{3-}$ ), total alkalinity (TA), bicarbonate concentration ( $HCO_3^-$ ), and aragonite saturation state ( $\Omega_{arag}$ ) of the artificial seawater (SW), specimens of the control (C), and the two treatments (T1, T2) are exposed to during the acclimation and experimental phase. In chapter 4.2, the response variables polyp extension, mass-specific respiration rate, and growth were described in detail and influences of abiotic parameters on the response variables were analyzed using bi- and multivariate analysis.

### 4.1 Seawater parameters

Results of the physical and chemical water parameters T, S,  $\sigma_\theta$ ,  $O_2$ , pH, nutrients, and TA, calculated  $HCO_3^-$  concentration and  $\Omega_{arag}$  are summarized in table 1 and described in detailed in the following subsections with respect to differences during acclimation and experimental phase.

Table 1 Summary of **A**) measured and **B**) calculated water parameter. Salinity (S) [PSU-scale], temperature (T) [°C] oxygen (O<sub>2</sub>) [mg L<sup>-1</sup>], pH, TA [μmol kg<sup>-1</sup> SW], the nutrients NO<sub>3</sub><sup>-</sup> [μmol kg<sup>-1</sup> SW], NO<sub>2</sub><sup>-</sup> [μmol kg<sup>-1</sup> SW], NH<sub>4</sub><sup>+</sup> [μmol kg<sup>-1</sup> SW], PO<sub>4</sub><sup>+</sup> [μmol kg<sup>-1</sup> SW], σ<sub>θ</sub>, HCO<sub>3</sub><sup>-</sup> [μmol kg<sup>-1</sup> SW], and Ω<sub>arag</sub> expressed in mean ± SD, for C, T1, and T2 during the acclimation and experimental phase.

<b>A</b>		<b>Measured parameter</b>								
<b>Phase</b>	<b>Treatment</b>	<b>S</b>	<b>T</b>	<b>Oxygen</b>	<b>pH</b>	<b>TA</b>	<b>NO<sub>3</sub><sup>-</sup></b>	<b>NO<sub>2</sub><sup>-</sup></b>	<b>NH<sub>4</sub><sup>+</sup></b>	<b>PO<sub>4</sub><sup>+</sup></b>
<b>Acclimation</b>	<b>C</b>	31.13 ± 0.20	11.01 ± 0.04	9.17 ± 0.16	8.14 ± 0.05	2752.44 ± 185.83	24.79 ± 20.70	0.19 ± 0.12	4.62 ± 8.35	0.13 ± 0.05
	<b>T1</b>	31.12 ± 0.17	11.23 ± 0.41	9.12 ± 0.11	8.14 ± 0.05	2865.14 ± 235.21	15.73 ± 15.56	0.66 ± 0.71	3.43 ± 1.96	0.15 ± 0.13
	<b>T2</b>	35.38 ± 2.31	11.24 ± 0.39	9.05 ± 0.15	8.17 ± 0.06	2994.11 ± 237.86	10.61 ± 8.44	0.34 ± 0.23	1.18 ± 1.18	0.46 ± 0.68
<b>Experiment</b>	<b>C</b>	31.05 ± 0.15	11.00 ± 0.06	9.23 ± 0.21	8.17 ± 0.03	2782.37 ± 56.95	3.14 ± 2.62	0.92 ± 1.23	3.29 ± 5.51	0.40 ± 0.32
	<b>T1</b>	31.06 ± 0.10	12.04 ± 0.08	9.07 ± 0.13	8.18 ± 0.03	2807.80 ± 81.22	3.49 ± 2.92	3.71 ± 5.54	2.93 ± 3.69	0.39 ± 0.34
	<b>T2</b>	38.04 ± 0.12	12.03 ± 0.09	9.01 ± 0.17	8.21 ± 0.03	3318.91 ± 52.91	4.02 ± 4.57	2.40 ± 1.17	8.99 ± 9.42	0.41 ± 0.33

<b>B</b>		<b>Calculated parameter</b>		
<b>Phase</b>	<b>Treatment</b>	<b>σ<sub>θ</sub></b>	<b>Ω<sub>arag</sub></b>	<b>HCO<sub>3</sub><sup>-</sup></b>
<b>Acclimation</b>	<b>C</b>	23.78 ± 0.15	2.92 ± 0.31	2222.89 ± 29.33
	<b>T1</b>	23.72 ± 0.18	3.02 ± 0.23	2226.96 ± 79.82
	<b>T2</b>	27.36 ± 1.80	3.99 ± 0.62	2473.00 ± 94.99
<b>Experiment</b>	<b>C</b>	23.73 ± 0.12	3.45 ± 0.19	2341.35 ± 64.73
	<b>T1</b>	23.55 ± 0.10	3.67 ± 0.15	2339.62 ± 87.68
	<b>T2</b>	29.00 ± 0.06	4.84 ± 0.33	2676.34 ± 32.52

During the acclimation phase (35 days, N= 29), the temperature of T1 and T2 was  $11.03 \pm 0.05$  °C and  $11.05 \pm 0.03$  °C, respectively, before the temperature was increased from  $\sim 11$  °C over two days to  $\sim 12$  °C. Once the final temperature was reached after the ramping, the temperature of T1 and T2 remained stable at an average of  $12.04 \pm 0.08$  °C and  $12.03 \pm 0.09$  °C, respectively, for 95.29 % and 94.87 % of the total duration of the experimental phase (50 days; N= 38). This minor difference was not significantly different (Wilcoxon test;  $p > 0.05$ ). The temperature of C was 95.15 % stable at an average of  $11.00 \pm 0.06$  °C for 85 days during the acclimation and experimental phase (Figure 9).

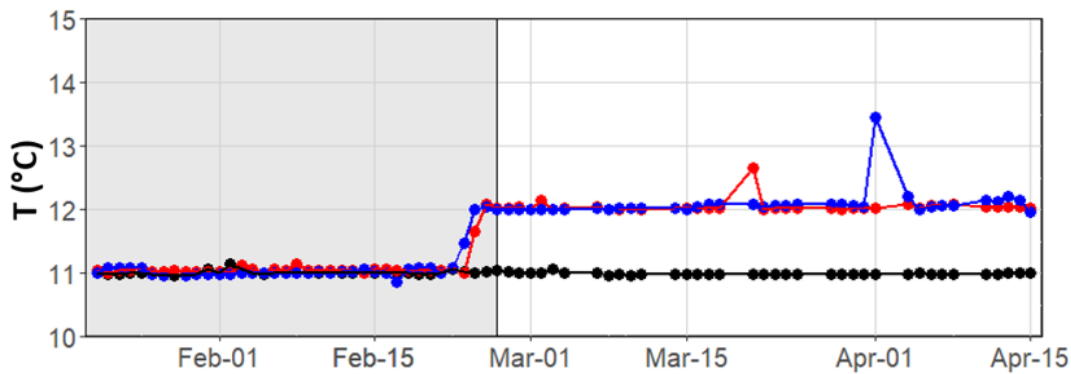


Figure 9: Daily average water temperature of the artificial seawater sampled from the treatment under Chilean salinity and temperature (C; black), Chilean salinity and Mediterranean temperature (T1; blue) and Mediterranean salinity and temperature (T2; red) during acclimation (grey background) and experimental phase (white background).

During the acclimation and experimental phases, the salinity values [PSU-scale] in the water tanks of C and T1 were  $31.07 \pm 0.19$  and  $31.10 \pm 0.16$ , respectively, and were not significantly different from each other (Wilcoxon test;  $p > 0.05$ ), while the salinity of T2 was gradually increased from 31 to 38 during the acclimation over 35 days (see chapter 3.3.2), stabilized at an average of  $38.04 \pm 0.12$  at the end of the acclimation phase and remaining constant during the experimental phase of 50 days (Fig. 10).

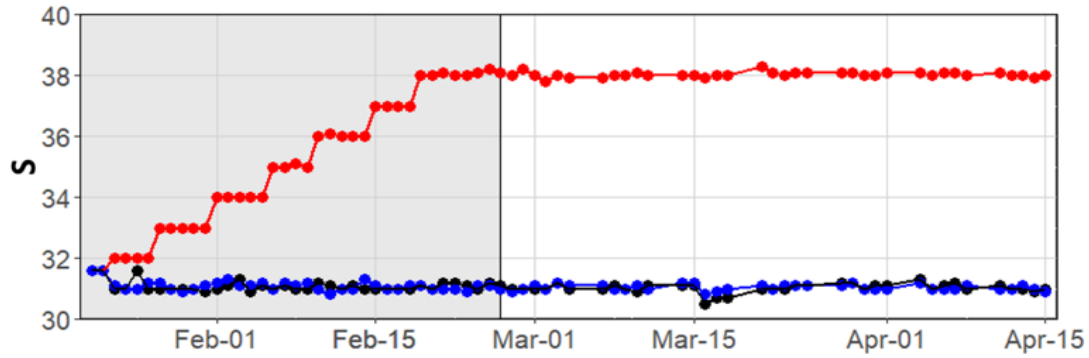


Figure 10: Daily salinity of the artificial seawater sampled from the treatment under Chilean salinity and temperature (C; black), Chilean salinity and Mediterranean temperature (T1; blue) and Mediterranean salinity and temperature (T2; red) during acclimation (grey background) and experimental phase (white background).

Sigma-Theta ( $\sigma_\theta$ ), calculated based on the recorded salinity and temperature, remained constant during the acclimation and experimental phase at an average of  $23.76 \pm 0.14$  (Wilcoxon test;  $p > 0.05$ ). Due to the manipulation of salinity and temperature during the T1 and T2 acclimation,  $\sigma_\theta$  in C as well as in T1 and T2 varied significantly between the acclimation and experimental phases (Wilcoxon test;  $p < 0.05$ ). The  $\sigma_\theta$  of T1 stabilized at  $23.54 \pm 0.09$ , while  $\sigma_\theta$  of T2 was characterized by an increased  $\sigma_\theta$  ( $29.00 \pm 0.07$ ) at the end of the acclimation period and during the duration of the experimental phase (Figure 11).

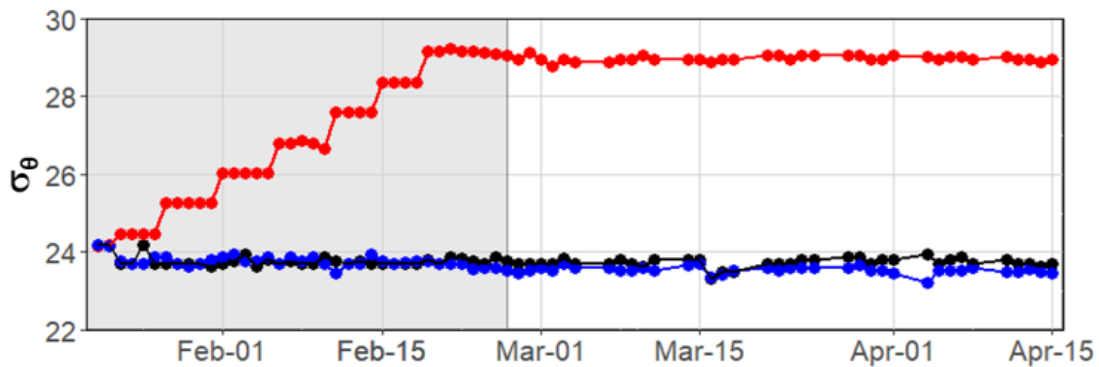


Figure 11: Calculated  $\sigma_\theta$  of the artificial seawater sampled from the treatment under Chilean salinity and temperature (C; black), Chilean salinity and Mediterranean temperature (T1; blue) and Mediterranean salinity and temperature (T2; red) during acclimation (grey background) and experimental phase (white background).

The oxygen concentration in C, T1, and T2 was stable at  $9.21 \pm 0.15$ ,  $9.08 \pm 0.14$ , and  $9.03 \pm 0.15$   $\text{mg L}^{-1}$ , respectively, and did not differ significantly between the acclimation ( $N = 29$ ) and experimental phases ( $N = 38$ ) (Kruskal-Wallis test;  $p > 0.05$ ) (Fig. 12).

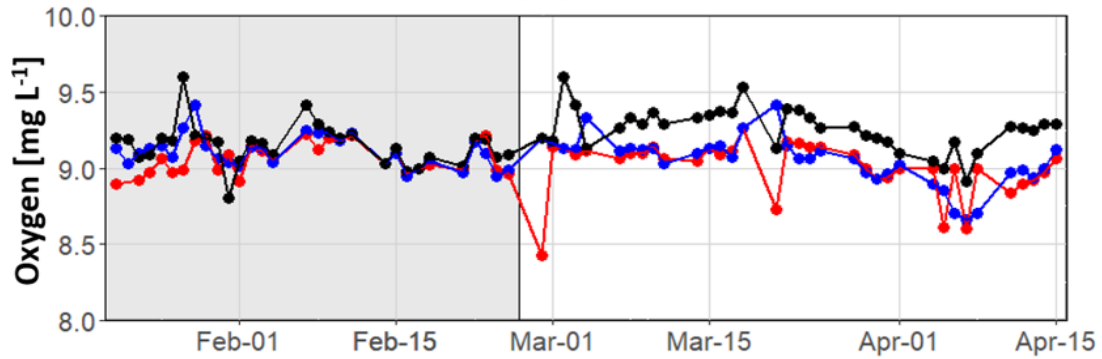


Figure 12: Daily oxygen concentration in mg L<sup>-1</sup> of the artificial seawater sampled from the treatment under Chilean salinity and temperature (C; black), Chilean salinity and Mediterranean temperature (T1; blue) and Mediterranean salinity and temperature (T2; red) during acclimation (grey background) and experimental phase (white background).

The pH of the water of C, T1, and T2 did not differ significantly during the acclimation (Kruskal-Wallis test;  $p > 0.05$ ), while the pH of C ( $8.17 \pm 0.03$ ), T1 ( $8.18 \pm 0.03$ ), and T2 ( $8.21 \pm 0.03$ ) varied significantly during the experimental phase (Wilcoxon test;  $p < 0.05$ ) (Fig. 13).

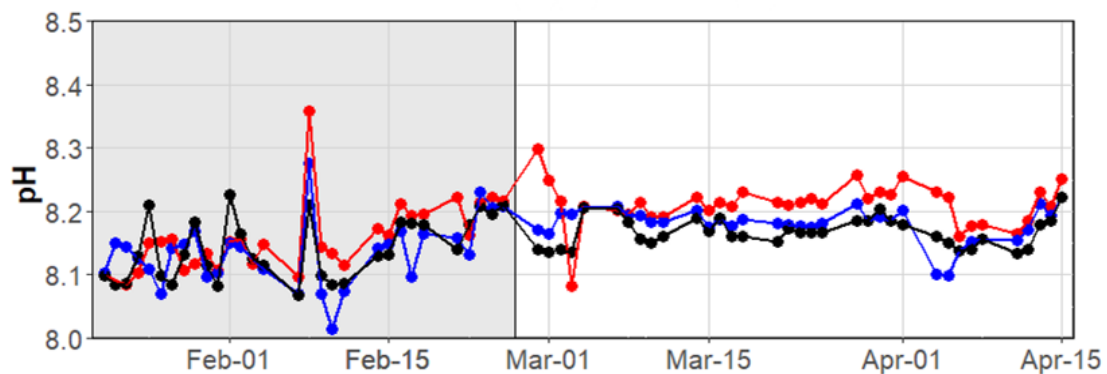


Figure 13: Daily pH of the artificial seawater sampled from the treatment under Chilean salinity and temperature (C; black), Chilean salinity and Mediterranean temperature (T1; blue) and Mediterranean salinity and temperature (T2; red) during acclimation (grey background) and experimental phase (white background).

Throughout the entire trial (acclimation and experimental phase), no significant differences were found between all treatments and the control in the concentration of  $\text{NO}_3^-$ ,  $\text{NH}_4^+$ ,  $\text{PO}_4^{4-}$ , and  $\text{NO}_2^-$  between T1 and T2 (Kruskal-Wallis test;  $p > 0.05$ ), while significant differences were recorded in  $\text{NO}_2^-$  in C compared to T1 and T2 (Kruskal-Wallis test;  $p < 0.05$ ). Nitrite concentration in C ( $0.69 \pm 1.04 \mu\text{mol kg}^{-1} \text{ SW}$ ) was significantly slightly lower compared to T1 ( $2.78 \pm 4.77 \mu\text{mol kg}^{-1} \text{ SW}$ ) and T2 ( $1.77 \pm 1.45 \mu\text{mol kg}^{-1} \text{ SW}$ ) (Fig. 14).

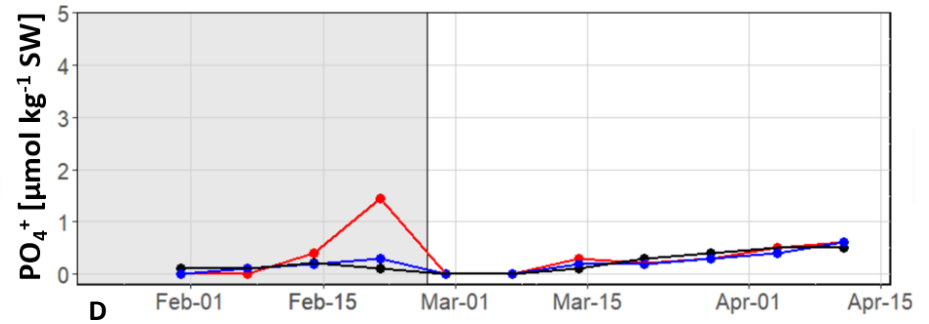
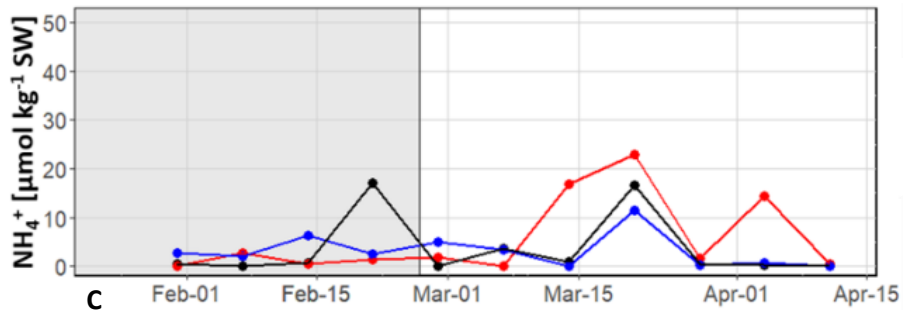
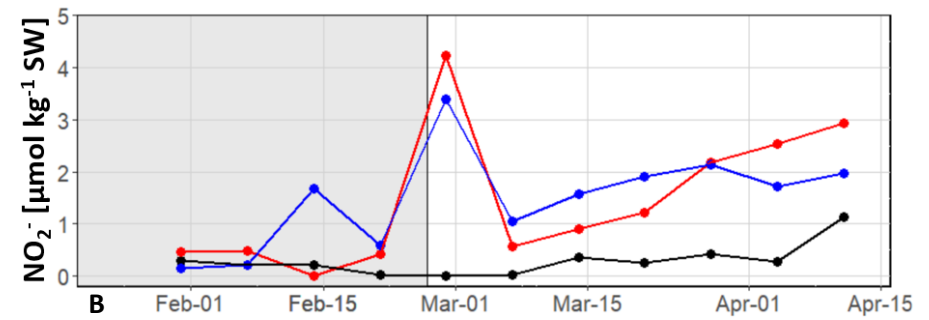
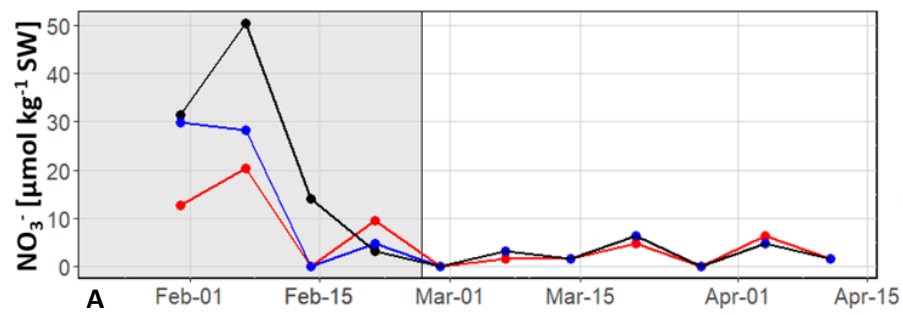


Figure 14: Weekly photometrically measured nitrate (A), nitrite (B), ammonium (C), and phosphate (D) concentration of the artificial seawater sampled from the treatment under Chilean salinity and temperature (C; black), Chilean salinity and Mediterranean temperature (T1; blue) and Mediterranean salinity and temperature (T2; red) during acclimation (grey background) and experimental phase (white background).

Control and treatment conditions differed in carbonate chemistry parameters with significantly higher TA (Wilcoxon test;  $p < 0.05$ ),  $\text{HCO}_3^-$  concentration and  $\Omega_{\text{arag}}$  in T2 (Tukey test;  $p < 0.05$ ) compared to T1 and C (Fig. 15).

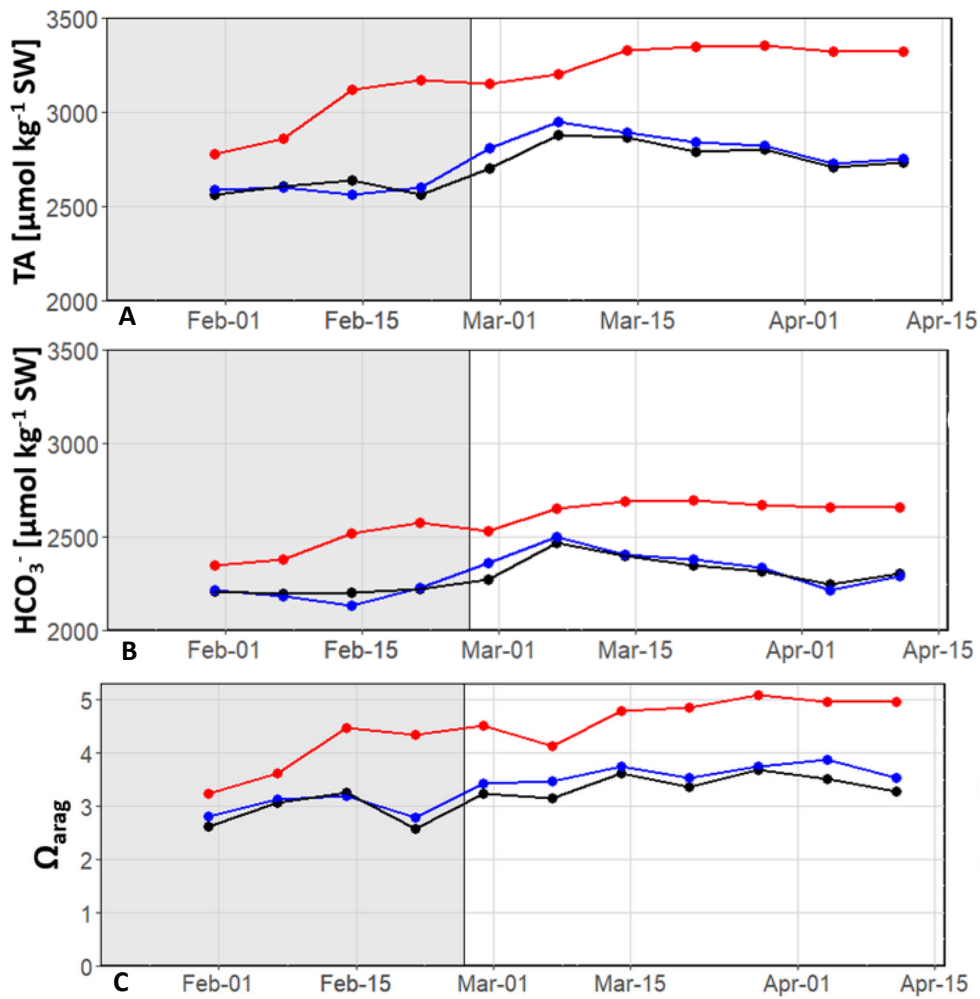


Figure 15: Weekly photometrically determined TA (A), calculated  $\text{HCO}_3^-$  concentration (B), and  $\Omega_{\text{arag}}$  (C) of the artificial seawater sampled from the treatment under Chilean salinity and temperature (C; black), Chilean salinity and Mediterranean temperature (T1; blue) and Mediterranean salinity and temperature (T2; red) during acclimation (grey background) and experimental phase (white background).

## 4.2 Response variables of the corals

No coral mortality was observed throughout acclimation and experimental phase under C, T1, and T2 conditions. In the following section the results of the polyp extension observations, the mass-specific respiration rate, and growth are described in detail during the acclimation and experimental phases.

### 4.2.1 Polyp extension

In the control and the two treatments, a high variation in the mean polyp expansion rate, evidenced by a high standard deviation, was observed both in the morning and in the evening. When comparing the mean polyp extension rate between C, T1, and T2, no significant differences were detected for the morning and evening observations (Kruskal-Wallis test;  $p > 0.05$ ) (Fig. 16).

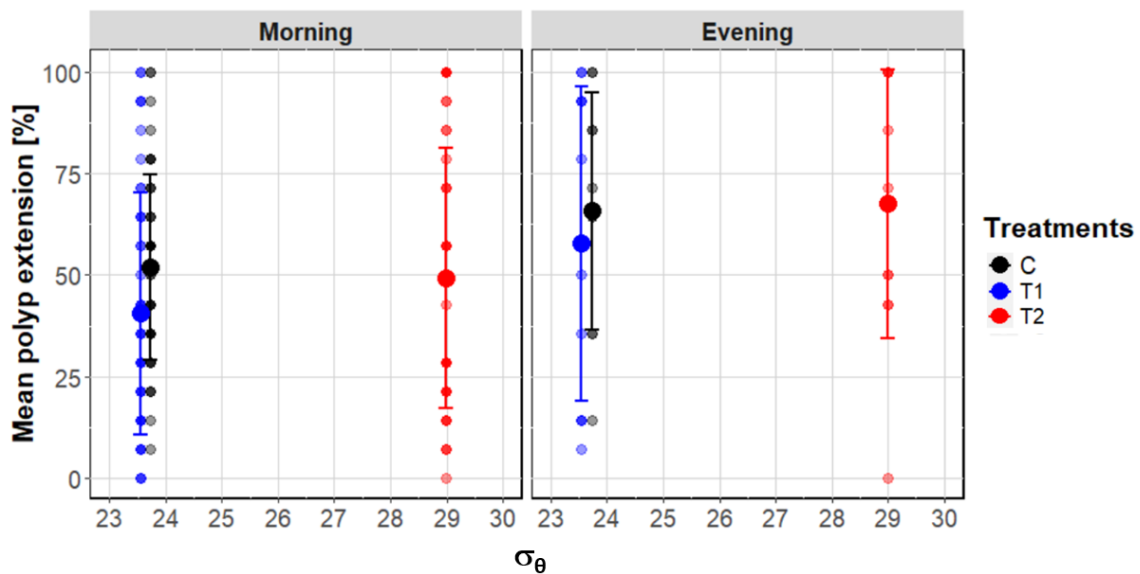


Figure 16: Mean polyp extension of *Desmophyllum dianthus* maintained under Chilean salinity and temperature (C; black), Chilean salinity and Mediterranean temperature (T1; blue) and Mediterranean salinity and temperature (T2; red), expressed in % of visible polyp extension rate related to mean  $\sigma_\theta$  for morning and evening observations, respectively. Significant differences are highlighted with asterisk \* for  $p < 0.05$ .

#### 4.2.2 Respiration

The comparison of the respiration rates served to identify changes in metabolic processes caused by external hyperthermal and -osmotic stress. No significant differences in the respiration rates between the corals maintained under C, T1, and T2 conditions were found after 3-days incubation to final conditions (Kruskal-Wallis test;  $p > 0.05$ ). This also holds true for the ones at the end of the 50-days experimental phase (ANOVA;  $p > 0.05$ ), as well as for the comparison of the data sets of the control and the treatments of the short- and the long-term exposure measurements (Kruskal-Wallis test;  $p > 0.05$ ) (Figure 17).

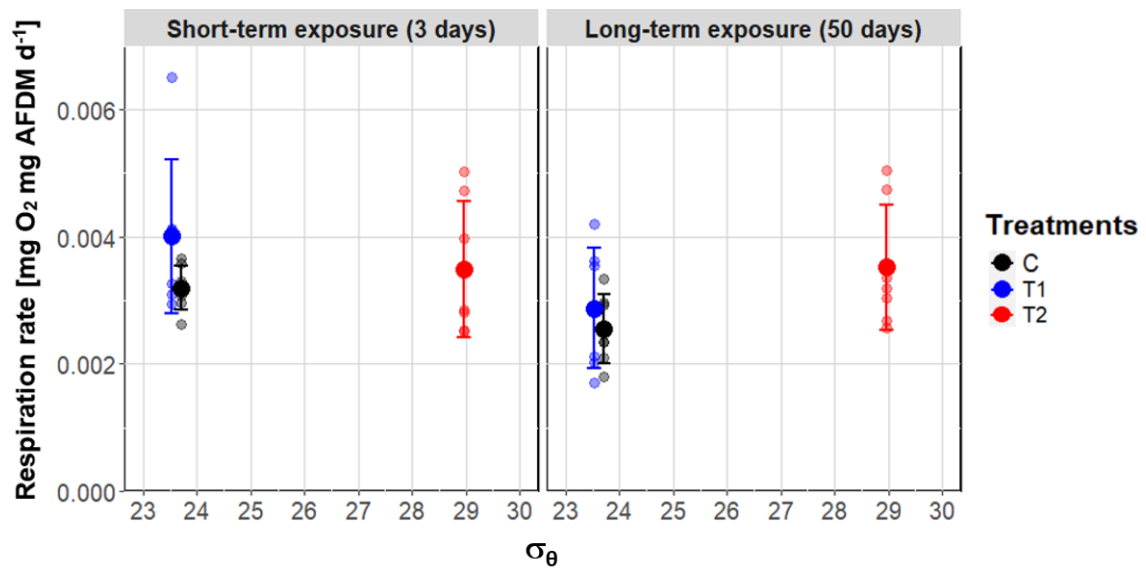


Figure 17: Respiration rate of *Desmophyllum dianthus* maintained under Chilean salinity and temperature (C; black), Chilean salinity and Mediterranean temperature (T1; blue) and Mediterranean salinity and temperature (T2; red), expressed in mg O<sub>2</sub> mg AFDM after the short-term exposure (3 days) and long-term exposure (50 days) related to  $\sigma_{\theta}$ . Significant differences are highlighted with asterisk \* for  $p < 0.05$ .

### 4.2.3 Growth

No significant differences in growth for the corals maintained under C ( $0.02 \pm 0.01 \text{ \% d}^{-1}$ ), T1 ( $0.03 \pm 0.03 \text{ \% d}^{-1}$ ) and T2 ( $0.02 \pm 0.03 \text{ \% d}^{-1}$ ) conditions were detected after the 35-days acclimation period (Kruskal-Wallis test;  $p > 0.05$ ). In contrast, significant differences in growth rates of C ( $0.02 \pm 0.01 \text{ \% d}^{-1}$ ), T1 ( $0.02 \pm 0.02 \text{ \% d}^{-1}$ ), and T2 ( $0.05 \pm 0.02 \text{ \% d}^{-1}$ ) were detected, exposed to 50-days incubation. A significant increase in the growth rates of corals maintained under T2 conditions was observed compared to the growth rates of corals maintained under C and T1 conditions (Wilcoxon test;  $p < 0.05$ ). On average, the growth of T2 corals was increased by  $0.0303 \text{ \% d}^{-1}$  (140 % inclination) in comparison to the mean growth rate of T1 corals during the experimental phase and C corals during the experimental phase and acclimation. Meanwhile, growth rate of corals only exposed to elevated temperature (T1) did not differ significantly from the ones maintained under C conditions (Kruskal-Wallis test;  $p > 0.05$ ) (Fig. 18).

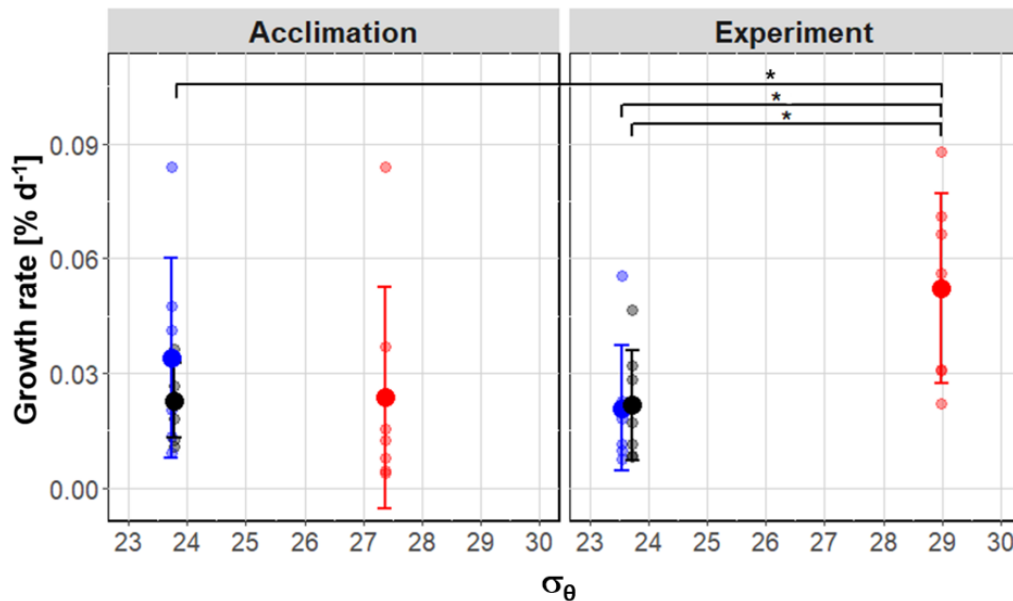


Figure 18: Growth rate of *Desmophyllum dianthus*' skeletal mass maintained under Chilean salinity and temperature (C; black), Chilean salinity and Mediterranean temperature (T1; blue) and Mediterranean salinity and temperature (T2; red), expressed in % per day during the acclimated (35 days) and experimental phase (50 days) under constant conditions related to  $\sigma_\theta$ . Significant differences are highlighted with asterisk \* for  $p < 0.05$ .

#### 4.2.4 Calyx area variation

No significant differences in calyx area between the C, T1, and T2 were found among acclimation and experimental phase (ANOVA;  $p > 0.05$ ). While in the acclimation growth rates of C ( $0.12 \pm 0.04 \% d^{-1}$ ), T1 ( $0.1 \pm 0.05 \% d^{-1}$ ), and T2 ( $0.14 \pm 0.08 \% d^{-1}$ ) were recorded, the experimental phase is characterized by degrowth rates in C ( $-0.08 \pm 0.06 \% d^{-1}$ ), T1 ( $-0.04 \pm 0.08 \% d^{-1}$ ), and T2 ( $-0.12 \pm 0.03 \% d^{-1}$ ). A negative significant reduction in calyx area was detected, comparing the mean growth rates of C, T1, and T2 of acclimation and experimental phase (ANOVA;  $p < 0.05$ ) (Fig. 19).

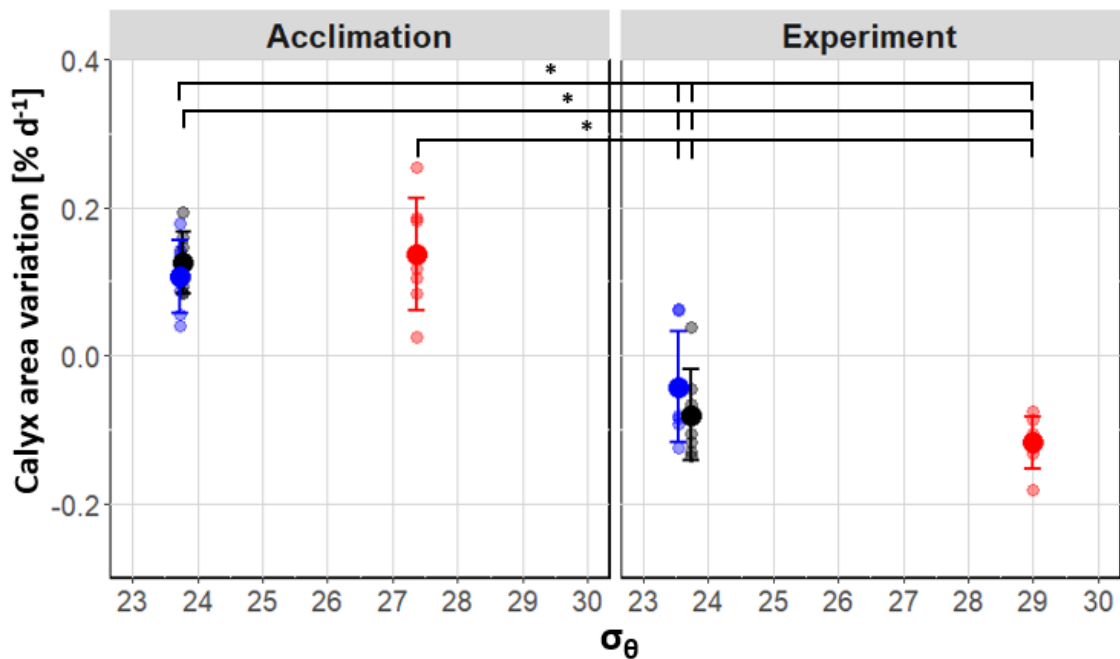


Figure 19: Growth rate of *Desmophyllum dianthus*' calyx area maintained under Chilean salinity and temperature (C; black), Chilean salinity and Mediterranean temperature (T1; blue), and Mediterranean salinity and temperature (T2; red), expressed in % per day during the acclimated (35 days) and experimental phase (50 days) under constant conditions related to  $\sigma_{\theta}$ . Significant differences are highlighted with asterisk \* for  $p < 0.05$ .

### 4.3 Multivariate analysis of water parameter and response variables

Multivariate analysis was performed to identify relationships between the measured seawater parameters during the acclimation (Table 2) and the experimental phase (Table 3). In the comparison of the Spearman rank correlation matrices of both incubation phases, a significant correlation between salinity and TA (acclimation: 0.61, experimental phase: 0.73;  $p < 0.05$ ) and between temperature and nitrite (acclimation: 0.71, experimental phase: 0.40;  $p < 0.05$ ) was found. Meanwhile, statistically relevant relationships were found between the water parameters shown in Table 2 and 3, which did not prevail across both incubation phases and therefore possess a low validity.

Table 2 Spearman rank correlation matrix of all measured seawater parameters (N = 12): Salinity, temperature [°C], pH, oxygen [mg L<sup>-1</sup>], NO<sub>3</sub><sup>-</sup> [μmol kg<sup>-1</sup> SW], NO<sub>2</sub><sup>-</sup> [μmol kg<sup>-1</sup> SW], NH<sub>4</sub><sup>+</sup> [μmol kg<sup>-1</sup> SW], PO<sub>4</sub><sup>-</sup> [μmol kg<sup>-1</sup> SW], and TA [μmol kg<sup>-1</sup> SW] during acclimation. A significant correlation coefficient  $\rho$  ( $p < 0.05$ ) is highlighted by an asterisk.

	S	T	pH	O <sub>2</sub>	NO <sub>3</sub> <sup>-</sup>	NO <sub>2</sub> <sup>-</sup>	NH <sub>4</sub> <sup>+</sup>	PO <sub>4</sub> <sup>-</sup>	TA
S	1.00								
T	0.30	1.00							
pH	0.12	0.09	1.00						
O <sub>2</sub>	0.06	-0.22	-0.61	1.00					
NO <sub>3</sub> <sup>-</sup>	0.07	-0.11	-0.86*	0.40	1.00				
NO <sub>2</sub> <sup>-</sup>	0.02	0.71*	0.10	-0.13	-0.14	1.00			
NH <sub>4</sub> <sup>+</sup>	-0.38	-0.08	0.21	-0.20	-0.33	0.16	1.00		
PO <sub>4</sub> <sup>-</sup>	0.01	0.15	0.63*	-0.42	-0.45	0.02	-0.17	1.00	
TA	0.61*	0.00	0.31	0.19	-0.11	-0.08	-0.49	0.31	1.00

Table 2 Spearman correlation rank matrix of measured seawater parameter (N = 27): Salinity, temperature [°C], pH, oxygen [mg L<sup>-1</sup>], NO<sub>3</sub><sup>-</sup> [μmol kg<sup>-1</sup> SW], NO<sub>2</sub><sup>-</sup> [μmol kg<sup>-1</sup> SW], NH<sub>4</sub><sup>+</sup> [μmol kg<sup>-1</sup> SW], PO<sub>4</sub><sup>-</sup> [μmol kg<sup>-1</sup> SW], and TA [μmol kg<sup>-1</sup> SW] during the experimental phase. A significant correlation coefficient  $\rho$  ( $p < 0.05$ ) is highlighted with an asterisk.

	S	T	pH	O <sub>2</sub>	NO <sub>3</sub> <sup>-</sup>	NO <sub>2</sub> <sup>-</sup>	NH <sub>4</sub> <sup>+</sup>	PO <sub>4</sub> <sup>-</sup>	TA
S	1.00								
T	0.35	1.00							
pH	0.41*	0.20	1.00						
O <sub>2</sub>	-0.61*	-0.66*	-0.21	1.00					
NO <sub>3</sub> <sup>-</sup>	-0.14	0.12	0.14	-0.04	1.00				
NO <sub>2</sub> <sup>-</sup>	0.13	0.40*	0.46*	-0.28	0.20	1.00			
NH <sub>4</sub> <sup>+</sup>	0.07	0.10	0.38*	-0.03	0.52*	0.26	1.00		
PO <sub>4</sub> <sup>-</sup>	-0.11	0.08	0.05	-0.15	0.58*	0.49*	0.10	1.00	
TA	0.73*	0.29	0.67*	-0.32	-0.04	0.26	0.39*	-0.18	1.00

In the analysis to determine the main factors influencing coral growth, the environmental parameters were tested for their correlation, including aragonite saturation instead of TA. A significant correlation was found between salinity ( $\rho = 0.76$ ;  $p < 0.05$ ) and growth during the acclimation phase (Supplementary material, Table S1). The same holds true for the aragonite saturation ( $\rho = 0.71$ ;  $p < 0.05$ ) and growth during the acclimation phase (Supplementary material, Table S1). The correlation between growth and salinity ( $\rho = 0.71$ ;  $p < 0.05$ ) or aragonite saturation ( $\rho = 0.60$ ;  $p < 0.05$ ) was confirmed in the longer experimental phase. Here the pH value ( $\rho = 0.43$ ;  $p < 0.05$ ) additionally significantly influenced growth (Supplementary material, Table S1).

## 5 Discussion

### 5.1 Polyp extension

*D. dianthus* specimens exposed only to elevated temperature (T1) and specimens exposed to multiple stressors (T2), namely increased temperature and salinity, exhibited no aberrant polyp behavior that differed from the activities of corals exposed to ambient Chilean salinity and temperature.

In this respect, 12 °C lies below the upper thermal tolerance limit of *D. dianthus*, above which polyp activity decreases and the polyp becomes inactive, e.g. observed for other CWC species (Previati *et al.*, 2010; Ferrier-Pagès *et al.*, 2012; Naumann *et al.* 2013; Gori *et al.*, 2015; Chapron *et al.*, 2021) and tropical scleractinian corals exposed to thermal stress (Howe and Marshall, 2001). The phenomenon that environmental stressors are visible in altered polyp activity has also been observed in octocorals . Mediterranean gorgonians, adapted to an average ambient temperature of 14 °C, exhibited an upper-temperature threshold between 18 °C and 20 °C, above which polyp activity was significantly reduced as a function of exposure duration (Previati *et al.*, 2010).

In addition to the temperature increase, the hyperosmotic condition does not affect the degree of polyp activity of *D. dianthus*. If corals are beyond their osmotic tolerance range, shrinkage or bulging of polyp tissue may occur, resulting in complete inactivation of the polyp (Jokiel *et al.* 1993). While a study to determine optimal cultivation conditions for the tropical scleractinian *Gonipora columna*, Ding *et al.* (2022) identified 30 - 35 [PSU-scale] as ideal salinities in which, the polyp exhibits an active behavior. In contrast at hypo- (25) and hyperosmotic conditions (40) the polyp was dysfunctional, observed as 0 % degree of open polyps. A similar response was observed by Jokiel *et al.* (1993) for tropical scleractinian *Pocillopora damicornis* and *Montipora*

*verrucosa* in Kaneohe Bay, part of the Hawaiian Archipelago, during a hypoosmotic stress event caused by storm floods. After the rapid decrease in salinity from 30 to 15 PSU, the polyps of both species became smaller and shrank until complete retraction resulted in a lethal effect for some organisms (Jokiel *et al.* 1993).

Visual inspection of high-resolution lateral and top images did not reveal any visible shrinkage or stretching. While the applied methodology defined polyp activity by the degree of polyp extension at two time points within a day, time-lapse photo series would allow investigation of the effects of temperature and salinity on the entire contraction-expansion cycles. The higher temporal resolution would enable examination of the dynamics of polyp movements for any changes in frequencies, which under natural conditions can affect the feeding rate and consequently control physiological performance (Naumann *et al.*, 2011). Information on the degree of polyp extension rate and cycle dynamics would provide detailed insights into changes in polyp behavior.

## 5.2 Respiration

Constant respiration rates in relation to temperature as the only parameter changed demonstrate that a 1 °C increase in temperature has no effect on the metabolism of *D. dianthus* specimens. No metabolic stress response is expected due to the naturally occurring annual temperature fluctuations of 8 to 13.5 in Comau Fjord (Försterra *et al.*, 2005; Beck *et al.*, 2022), where longer-term increases in water temperature of 12 °C can occur e.g. in winter (Laudien *et al.*, 2021).

That the average Mediterranean temperature provides optimal conditions for metabolic activities of *D. dianthus* was supported by studies that exposed various cosmopolitan CWCs to extreme thermal stress e.g., to identify upper thermal tolerance thresholds. The CWC *Dendrophyllia cornigera* exhibited constant metabolic rates at a temperature of 16 °C (Gori *et al.* 2014) and only increasing respiration rates at 20 °C (Reynauld *et al.*, 2021), compared to specimens exposed to an ambient temperature of 12 °C. A coral species, of the same genus (*Dendrophyllia ramea*), also occurring in the Mediterranean Sea exhibited increased respiration at a temperature of 24 °C, which it survived for two years in the laboratory. In contrast, other CWC such as *D. pertusum* and *M. oculata* already displayed altered respiration rates at temperature increases of + 2 °C and + 4 °C, respectively (Chapron *et al.*, 2021). As a result, thermal tolerance ranges depend strongly on the species. While in some studies respiration rates increase parallel with temperature (Coles and Jokiel, 1977), the phenomenon of constant respiration rates can be explained by a rapid increase in respiration rates which subsequently

returns to a basal level (Dorey *et al.*, 2020). Therefore, the temporal aspect can play a major role in the planning of measurement time points related to the species-specific metabolic responses. At the end of the two-year experiment of Reynaud *et al.* (2021), exposing *D. cornigera* and *D. ramea* to increased temperature a reduction in metabolic activity was observed. Meanwhile, in this study, the exposure duration of three months to increased temperature appears to not influence the metabolic response of the CWC *D. dianthus*.

*Desmophyllum dianthus* incubated under elevated temperature and hyperosmotic conditions, did not exhibit any deviation of the respiration rates during the duration of the experiment, compared to the specimens exposed to ambient temperature and salinity. A similar physiological effect was discovered by Colwin (2012), who tested the influence of different salinities below (22, 28) and above (42, 48) natural environmental conditions (35) (1 – 96 h) on the respiration rate of the tropical scleractinian coral *Acropora aspera* in an *ex-situ* experiment. While both hypersaline conditions induced no change in the respiration rate at any exposure duration, the respiration rate of both hyposaline conditions significantly increased compared to the control and it was positively related to exposure time, resulting in a 211% increase at a salinity of 22 for 96 h (Cowlin 2012). Scleractinian corals are more sensitive to short-term ( $\geq 12$  h) reduced salinity, while their metabolism is resistant even to highly elevated salinity over a longer period of three months (this study, Moberg *et al.* 1997, Cowlin 2012). While the combination of high temperature and high salinity did not exert any effect on the metabolism of *D. dianthus*, tropical scleractinian corals of eight genera (*Acropora*, *Echinopora*, *Galaxea*, *Montipora*, *Pocillopora*, *Psammacora*, *Stylpophora*, *Turbinaria*) exposed to elevated temperature and reduced salinity experienced a synergistic effect (Coles and Jokiel 1978; Xiubao *et al.*, 2009; Faxneld *et al.* 2010; Dias *et al.* 2019a). The synergistic effect resulted from an increase in metabolic rate due to the interaction of the temperature-induced increase in metabolism and the cost of osmoregulation, with hyposaline stress affecting corals more than thermal stress (Dias *et al.* 2019a).

In other marine invertebrates, different metabolic responses to osmotic stress have been identified. While salinity changes do not affect respiration rates of copepods (Svetlichny *et al.*, 2012), other osmoconformers such as Bivalvia and Echinodermata show lower respiration rates under hyposaline conditions and increased respiration rates under hypersaline conditions (Bouxin, 1931; Widdows, 1985; Navarro and González, 1998; Sarà *et al.* 2008; Shin *et al.* 2011; Yu *et al.* 2013). Reduced basal metabolic rate in marine invertebrates has been observed as a

common response to environmental stressors to survive until normal conditions return (Hand and Hardewig, 1996; Guppy and Withers 1999).

### 5.3. Growth

In addition to metabolic effects, corals respond to stressful environmental conditions with changes in their growth rate (Brown and Howard, 1985). The data obtained are essential for understanding the acclimation potential of *D. dianthus* and its capacity to maintain calcification rates under deviating salinity and temperature, such as those found in the Mediterranean (Coles and Jokiel, 1992; Porter *et al.*, 1999). Increased temperature and hyperosmotic condition stimulated the growth of *D. dianthus* by 140 % while the elevated temperature alone did not affect the growth rates. In the following sections, results are discussed regarding the impact of temperature, salinity, and the positively correlated seawater parameters  $\Omega_{\text{arag}}$  on the growth of scleractinian corals.

Temperature constitutes an important factor impacting coral growth. In this study, the growth rate of *D. dianthus* did not differ significantly at ambient and elevated temperature, which is within the range of the natural thermal variation in Comau Fjord (Fillinger and Richter 2013; Jantzen *et al.*, 2013b, Rossbach *et al.*, 2021). Similarly, the results of Naumann *et al.* (2013) show no significant growth differences between Mediterranean *D. dianthus* specimens exposed to the ambient temperature of 12 °C and to an elevated temperature of 17.5 °C. In contrast, growth rates of specimens of CWC *D. pertusum* collected from a nearshore Norwegian reef in the outer Trondheim Fjord, and therefore living under average colder temperatures of 8 °C, were already reduced at 12 °C (Büscher *et al.*, 2017). Consequently, the species-specific thermal tolerances of CWCs are also driven by habitat-related temperatures, which vary with latitude and increasing depth.

In contrast the results achieved for *D. dianthus*, investigations on tropical scleractinian corals have shown that a 1 °C increase in average temperature increases the growth rate by 3.1% by increasing the activity of enzymes involved in the calcification process until the upper thermal threshold is reached and the temperature negatively affects the organisms (Ip *et al.* 1991; Al-Horani *et al.*, 2003; Allemand *et al.*, 2004, 2011; McNeil *et al.*, 2004).

Therefore, the influence of temperature is highly species-specific, and *D. dianthus* can maintain its growth rate at average Mediterranean temperatures at least for 50 days, and even withstand

higher temperatures caused, for example, by climate change (Allemand *et al.*, 2010a, b; Naumann *et al.*, 2013).

Increased salinity compared to naturally occurring salinity had a positive effect on the growth of *D. dianthus* ( $p=0.71$ ). Few studies have been conducted to investigate the full osmotic tolerance range of corals. Ding *et al.* (2022) found slightly increased growth rates of specimens of the tropical scleractinian *Goripora columna* exposed to elevated salinity of 35 in comparison to corals maintained at a salinity of 30. Meanwhile, specimens exposed to extreme hypo- (25) and hypersaline conditions (40) exhibit a mortality rate of 100 %, which meant that growth rates could not be determined.

The slightly increased growth rates and high mortality at a salinity of 40 observed for *G. columna*, compared to the results of this study can be attributed to the different experimental designs (Ding *et al.*, 2022). Although the incubation time is approximately the same, the salinity was adjusted differently in the two studies. While in this study, salinity ramping preceded the experiment, Ding *et al.* (2022) increased salinity from 30 to 35 and 40 within one day. Therefore, the lack of acclimation may negatively affect calcification processes and therefore only a slightly increased skeletal growth was observed for the tropical scleractinian coral (Pandolfi *et al.*, 2010).

Other calcifying marine species, such as the invasive species *Brachidontes pharaonis* (Mollusca, Bivalvia) in the Mediterranean Sea, exhibit a steep incline in the growth of ~115 % from a salinity of 15 to the maximum value of 50, the growth rates decrease at even higher salinity (Sarà *et al.*, 2008). The stimulation of calcification processes can be affected by altered concentrations of ions, affecting the enzymatic functionality and therefore causing intracellular alterations of amino acid concentrations (Tedengren and Kautsky, 1986; Maar *et al.* 2015). As some amino acids are involved in the biomineralization process (Puverel *et al.*, 2005; Picker *et al.*, 2020), altered external osmotic conditions can impact the growth. An increased level of the prevalent skeletal amino acids, aspartic acid, can for example inhibit calcification of *Porites* spp. (Kellock *et al.*, 2020). Further studies are required to analyze the concentrations of amino acids, such as aspartic acid, in the coral tissue to determine their role in the calcification processes.

The significant correlation between the growth rates and the saturation state of aragonite during the experimental phase ( $p=0.60$ ) indicates that both are linked. While the *ex-situ* experiment correctly simulated the mean ambient temperature and salinity, the aragonite saturation stage of the artificial seawater exceeded the natural  $\Omega_{\text{arag}}$  range of Comau Fjord and the Mediterranean. The  $\Omega_{\text{arag}}$  increase by 40 % (+ 1.39) in the hyperosmotic treatment compared

to the control, presumably enables the corals to increase their growth rate. Therefore, corals exposed to elevated aragonite saturation favor skeletal formation. While growth rates of *D. dianthus* exposed to 4.84 aragonite saturation state showed a great increase in growth rates, *D. dianthus* specimens from the same Chilean population tested with the same  $\Omega_{\text{arag}}$  difference of + 1.4 but shifted slightly downward (1.31 and 2.79) showed no differences in growth (Martínez-Dios *et al.*, 2020).

Considering the results of Martínez-Dios *et al.* (2020) and of this study, the growth rates remain stable until a threshold between 3.45 and 4.84 is reached after which the growth rate sharply increases by 40 %. Therefore, no linear relationship between  $\Omega_{\text{arag}}$  and growth was found for the CWC *D. dianthus*, which contrasts with findings of the growth rates of the temperate coral *Astrangia poculata* (Holcom *et al.*, 2010) and tropical coral *Porites lutea* (Ohde *et al.*, 2004), which were tested in natural  $\Omega_{\text{arag}}$  until supersaturated conditions ( $\leq 7.77$ ) and whose growth increased linear with  $\Omega_{\text{arag}}$ . In other studies, the efficiency of the calcification process increased with increasing aragonite saturation state until a maximum capacity was reached, using the surrounding soluble aragonite, and the calcification rate remained constant with further elevated  $\Omega_{\text{arag}}$ . This trend, characterized by species-specific inclinations and thresholds, was found for tropical scleractinian corals *Favia fragum* (Cohen *et al.*, 2009; Putron *et al.*, 2011) and *Porites spp.* (Marubini *et al.*, 2001; Putron *et al.*, 2011). Large variations in calcification rates as a function of aragonite saturation suggest inter-specific differences in the calcification mechanism among corals and other calcifying organisms, such as bivalves, crustaceans, and gastropods, summarized in Ries *et al.* (2009).

*Desmophyllum dianthus* possesses the potential to grow faster under increased aragonite saturation and higher salinity resulting in the 140 % incline of growth rate. While in this study the increased aragonite saturation was due to increased salinity, Martínez-Dios *et al.* (2020) altered aragonite saturation by regulating pH via aeration with CO<sub>2</sub>-rich or CO<sub>2</sub>-depleted air which may affect calcification rates differently.

Due to the large natural variability of growth rates of *D. dianthus* found in Chilean populations driven by the rate of fluctuation and degree of natural disturbance, which occur is higher in the upper surface water rather than in the deep sea (Palma and Silva, 2004; Silva, 2008; Försterra *et al.*, 2005; Castro *et al.*, 2011; Fillinger and Richter, 2013; Beck *et al.*, 2022). Consequently, Beck *et al.* (2022) detected higher growth rates exceeding 0.2 % d<sup>-1</sup> in a depth of 300 m than in the shallow waters at 20 m, where *D. dianthus* growth rates were between 0 and 0.1 % d<sup>-1</sup>. Additional in situ growth is affected by food availability, which can, at least for a short term,

compensate the impact of stress events (Garcia-Herrera *et al.*, 2022), such as reduction of oxygen (Hanz *et al.*, 2019), acidification (Martínez-Dios *et al.*, 2020), and alterations in nutrient concentration (Langdon and Adkinson, 2005), and temperature (Puerta *et al.*, 2020). The high fluctuations of environmental parameters which also differ between benthic habitats in Comau Fjord (Silva, 2008) result in different growth rates of e.g.,  $< 0.1 \% d^{-1}$  (Beck *et al.*, 2022) and  $0.25 \% d^{-1}$  (Jantzen *et al.*, 2013b). Compared to the growth rates of *D. dianthus*, exposure to Chilean conditions is relatively low but still within the range of the natural growth rate occurring in Comau Fjord.

#### 5.4 Calyx area variation

During acclimation, no difference was observed between the calyx area of specimens of the control and both treatments, similar to the data obtained with the buoyant weight technique. In contrast, a reduction of the calyx area degrowth was observed for all specimens, regardless of their maintenance conditions after the experimental phase. While two treatments were exposed to deviant environmental conditions in the acclimation and experimental phase and therefore changes in radial growth may be expected, the control corals were exposed to the same conditions during both phases and should not show any changes, as for the other response variables.

Consequently, this methodology does not seem to be a reliable way to determine area changes of calyces of *D. dianthus*. One reason for this may be the generally slow calyx enlargement, as Försterra and Häussermann (2003) detected an average diameter increase of 1.6 mm per year in *D. dianthus* in their natural Chilean habitat, which is probably not accurately measurable in 50 days. Apart from the insufficiently detectable area changes, the methods introduce further sources of error in data acquisition and/or processing. Since the determination of calyx variation with the photo analytical software ImageJ produced meaningful results in the CWC *Caryophyllia huinayensis* (Fähse *et al.*, 2021), the source of error most likely lies in the process of data collection. In this regard, the error can originate from a variety of sources. The perpendicular alignment of the calyx surface to the camera is difficult, as the calyx, which is jagged by septa (Cairns *et al.*, 2005), is never fully aligned with the flat aquarium wall and a slightly different position can be expected each time the coral is repositioned. In addition, the image is captured through a total of three media; air, glass, and water, resulting a Snell's refraction effect that can distort a photographic image.

## 6 Conclusion

The study represents the first investigation exploring the synergistic effect of elevated temperature and salinity, in addition to increased temperature alone on the scleractinian CWC *D. dianthus*. Furthermore, this study represents the longest study testing the reaction of tropical and scleractinian cold-water corals to altered salinity and temperature conditions that deviate from their natural habitat. Osmotic stress is caused by fluctuating rainfall, evaporation, circulation, and freshwater inflow, usually lasting a few days up to weeks, however, the longest study to date testing warming and osmotic stress was conducted only over 10 days (Xiubao *et al.*, 2009).

During the three-month experimental period, no alterations in polyp extension or metabolic activity (i.e., respiration) were observed in either the uni- (higher temperature) or bifactorial (higher temperature and salinity) treatments. Growth of *D. dianthus* specimens exposed to increased temperature and salinity conditions was stimulated by the elevated salinity and aragonite saturation, while the tested slightly elevated temperature, which is within the natural range of seasonal variation in Comau Fjord (Försterra *et al.*, 2005), did not affect growth.

Presumably, the local population of *D. dianthus* in shallow waters of Comau Fjord exhibits great phenotypic plasticity to mild warming and significant hyperosmotic conditions. Due to the high plasticity of this ecosystem engineer, the entire ecosystem has an advantage over changes in environmental conditions caused by short-term stress events or longer-term impacts. Based on the acclimation potential of the local Chilean population, it may be concluded that the worldwide occurrence of this CWC is mainly due to the high phenotypic plasticity.

This study proves that a salinity of 38 does not negatively affect the physiological performance of *D. dianthus* and promotes the calcification rate. As salinity is a key factor driving the occurrence of CWCs, further studies need to be conducted to determine the full osmotic tolerance range of the scleractinian CWC *D. dianthus*, as Cowlin (2012) did for the tropical scleractinian *A. aspera*.

Furthermore, a cross-situ experiment with Chilean and Mediterranean *D. dianthus* specimens would provide information on general species-specific phenotypic plasticity or whether only Chilean *D. dianthus*, which naturally tolerate large fluctuations in their shallow habitat, exhibit a high acclimation potential.

## 7 Acknowledgements

First of all, I would like to thank my first supervisor Dr. Jürgen Laudien, who together with the team of the department "Benthic-Pelagic Processes" enabled the implementation of this study and supported me at any time during my work at AWI.

Additionally, I would like to thank my second supervisor Dr. Covadonga Orejas from the Instituto Español de Oceanografía (IEO-CSIC, Gijón, Spain), and who was based during my master thesis in the Hanse Wissenschafts Kolleg - Institute for Advanced study (Delmenhorst, Germany), for her continuous support and review, as well as my unofficial supervisor Dr. Marlene Wall and Kristina Beck for completing the team of supervisors and together expanding my knowledge of CWCs through their diverse and profound experiences and knowledge.

Finally, I would like to thank Thomas Heran, who collected the samples and thus enabled the execution of this laboratory experiment, and for providing his experience, especially in the field of photography.

Esther Lüdtke introduced me to the techniques and machines for analyzing TA and nutrient concentrations, and the food incubation method applied in this department.

Furthermore, a big thank you goes to my family, friends, my IMBRSea colleagues, and the students of room D2020 for the nice conversations.

The research leading to the results in this master thesis has received funding from the Alfred-Wegener-Institut Helmholtz-Zentrum für Polar- und Meeresforschung (programme 'Changing Earth – Sustaining our Future', Topic 4.2 and 6.1) and the European Union's Horizon 2020 research and innovation program under the project, grant agreement No 818123 (iAtlantic). This output reflects only the author's view and the European Union cannot be held responsible for any use that may be made of the information contained therein.

## 8 References

- Addamo, A. M.; Martínez-Baraldés, I.; Vertino, A.; López-González, P. J.; Taviani, M.; Machordom, A. (2015): Morphological polymorphism of *Desmophyllum dianthus* (Anthozoa: Hexacorallia) over a wide ecological and biogeographic range: stability in deep habitats? In *Zoologischer Anzeiger-A Journal of Comparative Zoology* 259, pp. 113–130.
- Al-Horani, F. A.; Al-Moghrabi, S. M.; Beer, D. de (2003): The mechanism of calcification and its relation to photosynthesis and respiration in the scleractinian coral *Galaxea fascicularis*. In *Marine Biology* 142 (3), pp. 419–426.
- Allemand, D.; Ferrier-Pagès, C.; Furla, P.; Houlbrèque, F.; Puverel, S.; Reynaud, S. et al. (2004): Biomineralisation in reef-building corals: from molecular mechanisms to environmental control. In *Comptes Rendus Palevol* 3 (6-7), pp. 453–467.
- Allemand, D.; Tambutté, É.; Zoccola, D.; Tambutté, S. (2011): Coral calcification, cells to reefs. In *Coral reefs: an ecosystem in transition*, pp. 119–150.
- Angeletti, L.; Taviani, M.; Canese, S.; Foglini, F.; Mastrototaro, F.; Argnani, A. et al. (2014): New deep-water cnidarian sites in the southern Adriatic Sea. In *Mediterranean Marine Science* 15 (2), pp. 263–273.
- Ballantyne, J. S.; Moon, T. W. (1986): The effects of urea, trimethylamine oxide and ionic strength on the oxidation of acyl carnitines by mitochondria isolated from the liver of the Little Skate *Raja erinacea*. In *Journal of Comparative Physiology B* 156 (6), pp. 845–851.
- Barnes, D. D. J.; Taylor, R. R. B.; Lough, J. J. M. (2001): Coral records. In: *The algorithmic beauty of seaweeds, sponges and corals*-pages: 163-168: Springer-Verlag.
- Beck, K. K.; Schmidt-Grieb, G. M.; Laudien, J.; Försterra, G.; Häussermann, V.; González, H. E. et al. (2022): Environmental stability and phenotypic plasticity benefit the cold-water coral *Desmophyllum dianthus* in an acidified fjord. In *Communications biology* 5 (1), pp. 1–12.
- Berkelmans, R.; Jones, A. M.; Schaffelke, B. (2012): Salinity thresholds of *Acropora* spp. on the Great Barrier Reef. In *Coral Reefs* 31 (4), pp. 1103–1110.
- Bouxin, H. (1931): Influence des variations rapides de la salinité sur la consommation d'oxygène chez *Mytilus edulis* var. galloprovincialis (Lmk.), par H. Bouxin: Institut Océanographique.
- Brooke, S.; Ross, S. W.; Bane, J. M.; Seim, H. E.; Young, C. M. (2013): Temperature tolerance of the deep-sea coral *Lophelia pertusa* from the southeastern United States. In *Deep Sea Research Part II: Topical Studies in Oceanography* 92, pp. 240–248. DOI: 10.1016/j.dsr2.2012.12.001.
- Brown, B. E.; Howard, L. S. (1985): Assessing the effects of “stress” on reef corals. In: *Advances in marine biology*, vol. 22: Elsevier, pp. 1–63.
- Buddemeier, R. W.; Kinzie, R. A. (1976): Coral growth. In *Oceanogr Mar Biol Annu Rev* 14, pp. 183–225.

Büscher, J. V.; Form, A. U.; Riebesell, U. (2017): Interactive effects of ocean acidification and warming on growth, fitness and survival of the cold-water coral *Lophelia pertusa* under different food availabilities. In *Frontiers in Marine Science* 4, p. 101.

Cairns, S. D. (1994): Scleractinia of the temperate North Pacific. In *Smithsonian Contributions to Zoology*.

Cairns, S. D. (1995): The marine fauna of New Zealand: Scleractinia (Cnidaria: Anthozoa). In *New Zealand Oceanographic Institute Memoir*.

Cairns, S. D. (2007): Deep-water corals: an overview with special reference to diversity and distribution of deep-water scleractinian corals. In *Bulletin of Marine Science* 81 (3), pp. 311–322.

Cairns, S. D.; Häussermann, V.; Försterra, G. (2005): A review of the Scleractinia (Cnidaria: Anthozoa) of Chile, with the description of two new species. In *Zootaxa* 1018 (1), pp. 15–46.

Carlier, A.; Le Guilloux, E.; Olu, K.; Sarrazin, J.; Mastrototaro, F.; Taviani, M.; Clavier, J. (2009): Trophic relationships in a deep Mediterranean cold-water coral bank (Santa Maria di Leuca, Ionian Sea). In *Marine Ecology Progress Series* 397, pp. 125–137.

Carreiro-Silva, M.; Cerqueira, T.; Godinho, A.; Caetano, M.; Santos, R. S.; Bettencourt, R. (2014): Molecular mechanisms underlying the physiological responses of the cold-water coral *Desmophyllum dianthus* to ocean acidification. In *Coral Reefs* 33 (2), pp. 465–476.

Castric-Fey, A. (1997): The Scleractinian *Dendrophyllia cornigera* in shallow water, at Ushant (Brittany, NE Atlantic), related to the absence of a thermic barrier. In *Oceanographic Literature Review* 5 (44), p. 491.

Castro, L. R.; Cáceres, M. A.; Silva, N.; Muñoz, M. I.; León, R.; Landaeta, M. F.; Soto-Mendoza, S. (2011): Short-term variations in mesozooplankton, ichthyoplankton, and nutrients associated with semi-diurnal tides in a patagonian Gulf. In *Continental Shelf Research* 31 (3-4), pp. 282–292.

Chapron, L.; Galand, P. E.; Pruski, A. M.; Peru, E.; Vétion, G.; Robin, S.; Lartaud, F. (2021): Resilience of cold-water coral holobionts to thermal stress. In *Proceedings of the Royal Society B* 288 (1965), p. 20212117.

Chimienti, G.; Bo, M.; Taviani, M.; Mastrototaro, F. (2018): Occurrence and Biogeography of Mediterranean Cold-Water Corals Mediterranean cold-water corals: Past, present and future, pp. 213–243. DOI: 10.1007/978-3-319-91608-8\_19.

Chui, A. P. Y.; Ang, P. (2015): Elevated temperature enhances normal early embryonic development in the coral *Platygyra acuta* under low salinity conditions. In *Coral Reefs* 34 (2), pp. 461–469.

Clausen, C. D.; Roth, A. A. (1975): Effect of temperature and temperature adaptation on calcification rate in the hermatypic coral *Pocillopora damicornis*. In *Marine Biology* 33 (2), pp. 93–100.

Cogswell, A. T.; Kenchington, E. L.R.; Lirette, C. G.; MacIsaac, K.; Best, M. M.; Li Beazley; Vickers, J. (2009): The Current State of Knowledge Concerning The Distribution of Coral in The Maritime Distribution of Coral in The Maritime Provinces Provinces Provinces.

Cohen, A. L.; McCorkle, D. C.; Putron, S. de; Gaetani, G. A.; Rose, K. A. (2009): Morphological and compositional changes in the skeletons of new coral recruits reared in acidified seawater: Insights into the biomineralization response to ocean acidification. In *Geochemistry, Geophysics, Geosystems* 10 (7).

Coles, S. L. (1992): Experimental comparison of salinity tolerances of reef corals from the Arabian Gulf and Hawaii: evidence for hyperhaline adaptation, pp. 227–234.

Coles, S. L.; Jokiel, P. L. (1977): Effects of temperature on photosynthesis and respiration in hermatypic corals. In *Marine Biology* 43 (3), pp. 209–216.

Coles, S. L.; Jokiel, P. L. (1978): Synergistic effects of temperature, salinity and light on the hermatypic coral *Montipora verrucosa*. In *Marine Biology* 49 (3), pp. 187–195.

Coles, S. L.; Jokiel, P. L. (1992): Effects of salinity on coral reefs In: Connell DW. In *Pollution in*.

Coles, S. L.; Jokiel, P. L. (2018): Effects of salinity on coral reefs. In: Pollution in tropical aquatic systems: CRC Press, pp. 147–166.

Cowlin, M. (2012): Osmoregulation and the anthozoan-dinoflagellate symbiosis.

Crossland, C. (1928): Ecology of the Reef-builders of Tahiti (3), pp. 717–735.

Davies, A. J.; Duineveld, G. C. A.; Lavaleye, M. S. S.; Bergman, M. J. N.; van Haren, H.; Roberts, J. M. (2009): Downwelling and deep-water bottom currents as food supply mechanisms to the cold-water coral *Lophelia pertusa* (Scleractinia) at the Mingulay Reef Complex. In *Limnology and Oceanography* 54 (2), pp. 620–629.

Davies, P. S. (1989): Short-term growth measurements of corals using an accurate buoyant weighing technique. In *Marine Biology* 101 (3), pp. 389–395.

Dias, M.; Ferreira, A.; Gouveia, R.; Vinagre, C. (2019a): Synergistic effects of warming and lower salinity on the asexual reproduction of reef-forming corals. In *Ecological Indicators* 98, pp. 334–348.

Dias, M.; Madeira, C.; Jogee, N.; Ferreira, A.; Gouveia, R.; Cabral, H. et al. (2019b): Oxidative stress on scleractinian coral fragments following exposure to high temperature and low salinity. In *Ecological Indicators* 107, p. 105586.

Ding, D.; Patel, A. K.; Singhanian, R. R.; Chen, C.; Dong, C. (2022): Effects of temperature and salinity on growth, metabolism and digestive enzymes synthesis of *Goniopora columna*. In *Biology* 11 (3), p. 436.

Dodds, L. A.; Roberts, J. M.; Taylor, A. C.; Marubini, F. (2007): Metabolic tolerance of the cold-water coral *Lophelia pertusa* (Scleractinia) to temperature and dissolved oxygen change. In *Journal of Experimental Marine Biology and Ecology* 349 (2), pp. 205–214.

Dorey, N.; Gjelsvik, Ø.; Kutti, T.; Büscher, J. V. (2020): Broad thermal tolerance in the cold-water coral *Lophelia pertusa* from Arctic and boreal reefs. In *Frontiers in physiology*, p. 1636.

Duineveld, G. C. A.; Jeffreys, R. M.; Lavaleye, M. S. S.; Davies, A. J.; Bergman, M. J. N.; Watmough, T.; Witbaard, R. (2012): Spatial and tidal variation in food supply to shallow cold-water coral reefs of the Mingulay Reef complex (Outer Hebrides, Scotland). In *Marine Ecology Progress Series* 444, pp. 97–115.

Duineveld, G. C. A.; Lavaleye, M. S. S.; Berghuis, E. M. (2004): Particle flux and food supply to a seamount cold-water coral community (Galicia Bank, NW Spain). In *Marine Ecology Progress Series* 277, pp. 13–23.

Duineveld, G. C. A.; Lavaleye, M. S. S.; Bergman, M. J. N.; Stigter, H. de; Mienis, F. (2007): Trophic structure of a cold-water coral mound community (Rockall Bank, NE Atlantic) in relation to the near-bottom particle supply and current regime. In *Bulletin of Marine Science* 81 (3), pp. 449–467.

Dullo, W.; Flögel, S.; Rüggeberg, A. (2008): Cold-water coral growth in relation to the hydrography of the Celtic and Nordic European continental margin. In *Marine Ecology Progress Series* 371, pp. 165–176.

Fähse, M. (2021): Cold-water corals and anthropogenic stressors – effects of sediment load on respiration, growth and behaviour of juvenile *Caryophyllia huinayensis*.

Faxneld, S.; Jörgensen, T. L.; Tedengren, M. (2010): Effects of elevated water temperature, reduced salinity and nutrient enrichment on the metabolism of the coral *Turbinaria mesenterina*. In *Estuarine, Coastal and Shelf Science* 88 (4), pp. 482–487.

Ferrier-Pagès, C.; Reynaud, S.; Allemand, D. (2012): Shallow water scleractinian corals of the Mediterranean Sea. In *Life in the Mediterranean Sea: a look at habitat changes: Nova Sciences Publishers, Inc*, pp. 387–422.

Fillinger, L.; Richter, C. (2013): Vertical and horizontal distribution of *Desmophyllum dianthus* in Comau Fjord, Chile: a cold-water coral thriving at low pH. In *PeerJ* 1, e194.

Fitt, W. K.; Brown, B. E.; Warner, M. E.; Dunne, R. P. (2001): Coral bleaching: interpretation of thermal tolerance limits and thermal thresholds in tropical corals. In *Coral Reefs* 20 (1), pp. 51–65.

Florin, M. (1962): La régulation isosmotique intracellulaire chez les invertébrés marins euryhalins. In *Bulletin de la Classe des Sciences/Académie Royale de Belgique* 48 (1), pp. 687–694.

Försterra, G.; Beuck, L.; Häussermann, V.; Freiwald, A. (2005): Shallow-water *Desmophyllum dianthus* (Scleractinia) from Chile: characteristics of the biocoenoses, the bioeroding community, heterotrophic interactions and (paleo)-bathymetric implications. In: *Cold-water corals and ecosystems: Springer*, pp. 937–977.

Försterra, G.; Häussermann, V. (2001): Large assemblages of azooxanthellate Scleractinia (Cnidaria: Anthozoa) in shallow waters of South Chilean fjords. In *Terra Nostra* 1 (6), p. 155.

Försterra, G.; Häussermann, V. (2003): First report on large scleractinian (Cnidaria: Anthozoa) accumulations in cold-temperate shallow water of south Chilean fjords. In *Zoologische Verhandlungen* 345, pp. 117–128.

Försterra, G.; Häussermann, V.; Laudien, J. (2016): Animal Forests in the Chilean fjords: discoveries, perspectives and threats in shallow and deep waters. In: *Marine Animal Forests*: Springer.

Freiwald, A.; Beuck, L.; Rüggeberg, A.; Taviani, M.; Hebbeln, D. (2009): The white coral community in the central Mediterranean Sea revealed by ROV surveys. In *Oceanography* 22 (1), pp. 58–74.

Freiwald, A.; Fossa, J. H.; Grehan, A.; Koslow, T.; Roberts, J. M. (2004): Cold-water coral reefs: out of sight-no longer out of mind: UNEP-WCMC.

Garcia-Herrera, N.; Cornils, A.; Laudien, J.; Niehoff, B.; Höfer, J.; Försterra, G. et al. (2022): Seasonal and diel variations in the vertical distribution, composition, abundance and biomass of zooplankton in a deep Chilean Patagonian Fjord. In *PeerJ* 10, e12823.

Gili, J.; Coma, R. (1998): Benthic suspension feeders: their paramount role in littoral marine food webs. In *Trends in ecology & evolution* 13 (8), pp. 316–321.

Gilles, R. (1973): Oxygen consumption as related to the amino-acid metabolism during osmoregulation in the blue crab *Callinectes sapidus*. In *Netherlands Journal of Sea Research* 7, pp. 280–289.

Goolish, E. M.; Burton, R. S. (1989): Energetics of osmoregulation in an intertidal copepod: Effects of anoxia and lipid reserves on the pattern of free amino acid accumulation. In *Functional Ecology*, pp. 81–89.

Goreau, T. F. (1964): Mass expulsion of zooxanthellae from Jamaican reef communities after Hurricane Flora. In *Science* 145 (3630), pp. 383–386.

Gori, A.; Ferrier-Pagès, C.; Hennige, S. J.; Murray, F.; Rottier, C.; Wicks, L. C.; Roberts, J. M. (2016): Physiological response of the cold-water coral *Desmophyllum dianthus* to thermal stress and ocean acidification. In *PeerJ* 4, e1606. DOI: 10.7717/peerj.1606.

Gori, A.; Reynaud, S.; Orejas, C.; Ferrier-Pagès, C. (2015): The influence of flow velocity and temperature on zooplankton capture rates by the cold-water coral *Dendrophyllia cornigera*. In *Journal of Experimental Marine Biology and Ecology* 466, pp. 92–97.

Gori, A.; Reynaud, S.; Orejas, C.; Gili, J.-M.; Ferrier-Pagès, C. (2014): Physiological performance of the cold-water coral *Dendrophyllia cornigera* reveals its preference for temperate environments. In *Coral Reefs* 33 (3), pp. 665–674.

Grange, K. R.; Singleton, R. I.; Richardson, J. R.; Hill, P. J.; Del Main, W. (1981): Shallow rock-wall biological associations of some southern fjords of New Zealand. In *New Zealand journal of zoology* 8 (2), pp. 209–227.

Guinotte, J. M.; Orr, J.; Cairns, S. D.; Freiwald, A.; Morgan, L.; George, R. (2006): Climate change and deep-sea corals: will chemical and physical changes in the world's oceans alter the distribution of deep-sea bioherm-forming scleractinians. In *Front. Ecol. Environ* 3, pp. 141–146.

Guppy, M.; Withers, P. (1999): Metabolic depression in animals: physiological perspectives and biochemical generalizations. In *Biological Reviews* 74 (1), pp. 1–40.

Hand, S. C.; Hardewig, I. (1996): Downregulation of Cellular Metabolism During Environmental Stress: Mechanisms and Implications. In *Annual Review of Physiology* 58 (1), pp. 539–563. DOI: 10.1146/annurev.ph.58.030196.002543.

Hanz, U.; Wienberg, C.; Hebbeln, D.; Duineveld, G.; Lavaleye, M.; Juva, K. et al. (2019): Environmental factors influencing benthic communities in the oxygen minimum zones on the Angolan and Namibian margins. In *Biogeosciences* 16 (22), pp. 4337–4356.

Häussermann, V.; Försterra, G. (2007): Large assemblages of cold-water corals in Chile: a summary of recent findings and potential impacts. In *Bulletin of Marine Science* 81 (3), pp. 195–207.

Hochachka, P. W.; Somero, G. N. (2002): Biochemical adaptation: mechanism and process in physiological evolution: Oxford university press.

Hoegh-Guldberg, O. (2014): Coral reef sustainability through adaptation: glimmer of hope or persistent mirage? In *Current Opinion in Environmental Sustainability* 7, pp. 127–133.

Hoegh-Guldberg, O.; Mumby, P. J.; Hooten, A. J.; Steneck, R. S.; Greenfield, P.; Gomez, E. et al. (2007): Coral reefs under rapid climate change and ocean acidification. In *Science* 318 (5857), pp. 1737–1742.

Hofmann, G. E.; Todgham, A. E. (2010): Living in the now: physiological mechanisms to tolerate a rapidly changing environment. In *Annu Rev Physiol* 72 (1), pp. 127–145.

Holcomb, M.; McCorkle, D. C.; Cohen, A. L. (2010): Long-term effects of nutrient and CO<sub>2</sub> enrichment on the temperate coral *Astrangia poculata* (Ellis and Solander, 1786). In *Journal of Experimental Marine Biology and Ecology* 386 (1-2), pp. 27–33.

Howe, S. A.; Marshall, A. T. (2001): Thermal compensation of metabolism in the temperate coral, *Plesiastrea versipora* (Lamarck, 1816). In *Journal of Experimental Marine Biology and Ecology* 259 (2), pp. 231–248.

Howe, S. A.; Marshall, A. T. (2002): Temperature effects on calcification rate and skeletal deposition in the temperate coral, *Plesiastrea versipora* (Lamarck). In *Journal of Experimental Marine Biology and Ecology* 275 (1), pp. 63–81.

Humphrey, C.; Weber, M.; Lott, C.; Cooper, T.; Fabricius, K. J. C. R. (2008): Effects of suspended sediments, dissolved inorganic nutrients and salinity on fertilisation and embryo development in the coral *Acropora millepora* (Ehrenberg, 1834). In *Coral Reefs* 27 (4), pp. 837–850.

Ip, Y. K.; Krishnaveni, P. (1991): Incorporation of strontium (90Sr<sup>2+</sup>) into the skeleton of the hermatypic coral *Galaxea fascicularis*. In *Journal of Experimental Zoology* 258 (2), pp. 273–276.

Jahnke, L. S.; White, A. L. (2003): Long-term hyposaline and hypersaline stresses produce distinct antioxidant responses in the marine alga *Dunaliella tertiolecta*. In *Journal of Plant Physiology* 160 (10), pp. 1193–1202.

Jantzen, C.; Häussermann, V.; Försterra, G.; Laudien, J.; Ardelan, M.; Maier, S.; Richter, C. (2013a): Occurrence of a cold-water coral along natural pH gradients (Patagonia, Chile). In *Marine Biology* 160 (10), pp. 2597–2607.

Jantzen, C.; Laudien, J.; Sokol, S.; Försterra, G.; Häussermann, V.; Kupprat, F.; Richter, C. (2013b): In situ short-term growth rates of a cold-water coral. In *Marine and Freshwater Research* 64 (7), pp. 631–641.

Jokiel, P.; Maragos, J.; Franzisket, L. (1978): Coral growth: buoyant weight technique in Coral reefs: research methods (ed. Stoddart, D. & Johannes, RE) 529–542: UNESCO.

Jokiel, P. L.; Hunter, C. L.; Taguchi, S.; Watarai, L. (1993): Ecological impact of a fresh-water “reef kill” in Kaneohe Bay, Oahu, Hawaii. In *Coral Reefs* 12 (3), pp. 177–184.

Kellock, C.; Cole, C.; Penkman, K.; Evans, D.; Kröger, R.; Hintz, C. et al. (2020): The role of aspartic acid in reducing coral calcification under ocean acidification conditions. In *Scientific reports* 10 (1), pp. 1–8.

Klein, B.; Roether, W.; Manca, B. B.; Bregant, D.; Beitzel, V.; Kovacevic, V.; Luchetta, A. (1999): The large deep water transient in the Eastern Mediterranean. In *Deep Sea Research Part I: Oceanographic Research Papers* 46 (3), pp. 371–414.

Komsta, L. (2022): outliers: Tests for outliers. In *R package version 0.15*. Available online at <https://CRAN.R-project.org/package=outliers>.

Kuanui, P.; Chavanich, S.; Viyakarn, V.; Omori, M.; Lin, C. (2015): Effects of temperature and salinity on survival rate of cultured corals and photosynthetic efficiency of zooxanthellae in coral tissues. In *Ocean Science Journal* 50 (2), pp. 263–268.

Lang, F.; Busch, G. L.; Ritter, M.; Volkl, H.; Waldegger, S.; Gulbins, E.; Haussinger, D. (1998): Functional significance of cell volume regulatory mechanisms. In *Physiological reviews* 78 (1), pp. 247–306.

Langdon, C.; Atkinson, M. J. (2005): Effect of elevated pCO<sub>2</sub> on photosynthesis and calcification of corals and interactions with seasonal change in temperature/irradiance and nutrient enrichment. In *Journal of Geophysical Research: Oceans* 110 (C9).

Laudien, J.; Häussermann, V.; Försterra, G.; Heran, T. (2021): Water temperature at time series station X-Huinay, Comau Fjord, Patagonia, Chile in 2017/2018. With assistance of Alfred Wegener Institute, Helmholtz Centre for Polar and Marine Research, Bremerhaven.

Lirman, D.; Manzello, D. (2009): Patterns of resistance and resilience of the stress-tolerant coral *Siderastrea radians* (Pallas) to sub-optimal salinity and sediment burial. In *Journal of Experimental Marine Biology and Ecology* 369 (1), pp. 72–77.

Lough, J. M.; Barnes, D. J. (1997): Several centuries of variation in skeletal extension, density and calcification in massive *Porites* colonies from the Great Barrier Reef: a proxy for seawater temperature and a background of variability against which to identify unnatural change. In *Journal of Experimental Marine Biology and Ecology* 211 (1), pp. 29–67.

Maar, M.; Saurel, C.; Landes, A.; Dolmer, P.; Petersen, J. K. (2015): Growth potential of blue mussels (*M. edulis*) exposed to different salinities evaluated by a Dynamic Energy Budget model. In *Journal of Marine Systems* 148, pp. 48–55.

Maeda, M.; Thompson, G. A. (1986): On the mechanism of rapid plasma membrane and chloroplast envelope expansion in *Dunaliella salina* exposed to hypoosmotic shock. In *The Journal of cell biology* 102 (1), pp. 289–297.

Manzello, D.; Lirman, D. (2003): The photosynthetic resilience of *Porites furcata* to salinity disturbance. In *Coral Reefs* 22 (4), pp. 537–540.

Martínez-Dios, A.; Pelejero, C.; López-Sanz, À.; Sherrell, R. M.; Ko, S.; Häussermann, V. et al. (2020): Effects of low pH and feeding on calcification rates of the cold-water coral *Desmophyllum dianthus*. In *PeerJ* 8, e8236.

Marubini, Francesca; Barnett, H.; Langdon, C.; Atkinson, M. J. (2001): Dependence of calcification on light and carbonate ion concentration for the hermatypic coral *Porites compressa*. In *Marine Ecology Progress Series* 220, pp. 153–162.

Massel, S. R. (2015): *Internal Gravity Waves in the Shallow Seas*. Cham: Springer International Publishing AG (GeoPlanet). Available online at <https://ebookcentral.proquest.com/lib/kxp/detail.action?docID=3567617>.

Mayfield, A. B.; Gates, R. D. (2007): Osmoregulation in anthozoan–dinoflagellate symbiosis. In *Comparative Biochemistry and Physiology Part A: Molecular & Integrative Physiology* 147 (1), pp. 1–10.

McNeil, B. I.; Matear, R. J.; Barnes, D. J. (2004): Coral reef calcification and climate change: The effect of ocean warming. In *Geophysical Research Letters* 31 (22).

Mienis, F.; Stigter, H. C. de; White, M.; Duineveld, G.; Haas, H. de; van Weering, T. C.E. (2007): Hydrodynamic controls on cold-water coral growth and carbonate-mound development at the SW and SE Rockall Trough Margin, NE Atlantic Ocean. In *Deep Sea Research Part I: Oceanographic Research Papers* 54 (9), pp. 1655–1674.

Millero, F. J.; Morse, J.; Chen, C. (1979): The carbonate system in the western Mediterranean Sea. In *Deep Sea Research Part A. Oceanographic Research Papers* 26 (12), pp. 1395–1404.

Moberg, F.; Nyström, M.; Kautsky, N.; Tedengren, M.; Jarayabhand, P. (1997): Effects of reduced salinity on the rates of photosynthesis and respiration in the hermatypic corals *Porites lutea* and *Pocillopora damicornis*. In *Marine Ecology Progress Series* 157, pp. 53–59.

Morse, J. W.; Arvidson, R. S.; Lüttge, A. (2007): Calcium carbonate formation and dissolution. In *Chemical reviews* 107 (2), pp. 342–381.

Moulton, T. L. (2018): rMR: Importing data from Loligo Systems software, calculating metabolic rates and critical tensions. In *R package, version 1* (0).

Movilla, J.; Orejas, C.; Calvo, E.; Gori, A.; López-Sanz, À.; Grinyó, J. et al. (2014): Differential response of two Mediterranean cold-water coral species to ocean acidification. In *Coral Reefs* 33 (3), pp. 675–686.

Muehllehner, N.; Edmunds, P. J. (2008): Effects of ocean acidification and increased temperature on skeletal growth of two scleractinian corals, *Pocillopora meandrina* and *Porites rus* 7.

Naumann, M. S.; Orejas, C.; Ferrier-Pagès, C. (2013): High thermal tolerance of two Mediterranean cold-water coral species maintained in aquaria. In *Coral Reefs* 32 (3), pp. 749–754.

Naumann, M. S.; Orejas, C.; Ferrier-Pagès, C. (2014): Species-specific physiological response by the cold-water corals *Lophelia pertusa* and *Madrepora oculata* to variations within their natural temperature range. In *Deep Sea Research Part II: Topical Studies in Oceanography* 99, pp. 36–41.

Naumann, M. S.; Orejas, C.; Wild, C.; Ferrier-Pagès, C. (2011): First evidence for zooplankton feeding sustaining key physiological processes in a scleractinian cold-water coral. In *Journal of Experimental Biology* 214 (21), pp. 3570–3576.

Navarro, J. M.; Gonzalez, C. M. (1998): Physiological responses of the Chilean scallop *Argopecten purpuratus* to decreasing salinities. In *Aquaculture* 167 (3), pp. 315–327. DOI: 10.1016/S0044-8486(98)00310-X.

Normant, M.; Lamprecht, I. (2006): Does scope for growth change as a result of salinity stress in the amphipod *Gammarus oceanicus*? In *Journal of Experimental Marine Biology and Ecology* 334 (1), pp. 158–163.

Ohde, S.; Hossain, M. M. M. (2004): Effect of CaCO<sub>3</sub> (aragonite) saturation state of seawater on calcification of *Porites* coral. In *Geochemical Journal* 38 (6), pp. 613–621.

Orejas, C.; Ferrier-Pagès, C.; Reynaud, S.; Gori, A.; Beraud, E.; Tsounis, G. et al. (2011a): Long-term growth rates of four Mediterranean cold-water coral species maintained in aquaria. In *Marine Ecology Progress Series* 429, pp. 57–65.

Orejas, C.; Ferrier-Pagès, C.; Reynaud, S.; Tsounis, G.; Allemand, D.; Gili, J. M. (2011b): Experimental comparison of skeletal growth rates in the cold-water coral *Madrepora oculata* Linnaeus, 1758 and three tropical scleractinian corals. In *Journal of Experimental Marine Biology and Ecology* 405 (1-2), pp. 1–5.

Orejas, C.; Jiménez, C. (Eds.) (2019): Mediterranean Cold-Water Corals: Past, Present and Future: Understanding the Deep-Sea Realms of Coral. Cham: Springer International Publishing.

Oren, A. (1999): Bioenergetic aspects of halophilism. In *Microbiology and molecular biology reviews* 63 (2), pp. 334–348.

Palanques, A.; Madron, X. D.; Puig, P.; Fabres, J.; Guillén, J.; Calafat, A. et al. (2006): Suspended sediment fluxes and transport processes in the Gulf of Lions submarine canyons. The role of storms and dense water cascading. In *Marine Geology* 234 (1-4), pp. 43–61.

Palma, S.; Silva, N. (2004): Distribution of siphonophores, chaetognaths, euphausiids and oceanographic conditions in the fjords and channels of southern Chile. In *Deep Sea Research Part II: Topical Studies in Oceanography* 51 (6), pp. 513–535. DOI: 10.1016/j.dsr2.2004.05.001.

Picker, A.; Kellermeier, M.; Seto, J.; Gebauer, D.; Cölfen, H. (2012): The multiple effects of amino acids on the early stages of calcium carbonate crystallization. In *Zeitschrift für Kristallographie-Crystalline Materials* 227 (11), pp. 744–757.

Pierrot, D.; Lewis, E.; Wallace, D. W. R. (2006): MS Excel program developed for CO<sub>2</sub> system calculations. In *ORNL/CDIAC-105a. Carbon dioxide information analysis center, oak ridge national laboratory, US Department of Energy, Oak Ridge, Tennessee* 10.

Porter, J. W.; Lewis, S. K.; Porter, K. G. (1999): The effect of multiple stressors on the Florida Keys coral reef ecosystem: a landscape hypothesis and a physiological test. In *Limnology and Oceanography* 44 (3part2), pp. 941–949.

Previati, M.; Scinto, A.; Cerrano, C.; Osinga, R. (2010): Oxygen consumption in Mediterranean octocorals under different temperatures. In *Journal of Experimental Marine Biology and Ecology* 390 (1), pp. 39–48.

Puerta, P.; Johnson, C.; Carreiro-Silva, M.; Henry, L.; Kenchington, E.; Morato, T. et al. (2020): Influence of water masses on the biodiversity and biogeography of deep-sea benthic ecosystems in the North Atlantic. In *Frontiers in Marine Science*, p. 239.

Putron, S. J.; McCorkle, D. C.; Cohen, A. L.; Dillon, A. B. (2011): The impact of seawater saturation state and bicarbonate ion concentration on calcification by new recruits of two Atlantic corals. In *Coral Reefs* 30 (2), pp. 321–328.

Puverel, S.; Tambutté, E.; Pereira-Mouriès, L.; Zoccola, D.; Allemand, Denis; Tambutté, S. (2005): Soluble organic matrix of two Scleractinian corals: partial and comparative analysis. In *Comparative Biochemistry and Physiology Part B: Biochemistry and Molecular Biology* 141 (4), pp. 480–487.

R Core Team (2021): R: A language and environment for statistical computing. R Foundation for Statistical Computing, Vienna, Austria. In <http://www.R-project.org>.

Reynaud, S.; Orejas, C.; Campagno, A.; Rottier, C.; Jimenez, C.; Ferrier-Pagès, C. (2021): Dendrophylliidae cold-water corals in a warm ocean: the effect of exposure duration on their physiological response. In *Deep Sea Research Part II: Topical Studies in Oceanography* 193, p. 104962.

Ries, J. B.; Cohen, A. L.; McCorkle, D. C. (2009): Marine calcifiers exhibit mixed responses to CO<sub>2</sub>-induced ocean acidification. In *Geology* 37 (12), pp. 1131–1134.

Risk, M. J.; Heikoop, J. M.; Snow, M. G.; Beukens, R. (2002): Lifespans and growth patterns of two deep-sea corals: *Primnoa resedaeformis* and *Desmophyllum cristagalli*. In *Hydrobiologia* 471 (1), pp. 125–131.

Roberts, J. M.; Wheeler, A.; Freiwald, A.; Cairns, S. (2009): Cold-water corals: the biology and geology of deep-sea coral habitats: Cambridge University Press.

Roberts, J. M.; Wheeler, A. J.; Freiwald, A. (2006): Reefs of the deep: the biology and geology of cold-water coral ecosystems. In *Science* 312 (5773), pp. 543–547.

Rosbach, S.; Rosbach, F. I.; Häussermann, V.; Försterra, G.; Laudien, J. (2021): In situ Skeletal Growth Rates of the Solitary Cold-Water Coral *Tethocyathus endesa* From the Chilean Fjord Region. In *Frontiers in Marine Science* 8 (757702).

Sarà, G.; Romano, C.; Widdows, J.; Staff, F. J. (2008): Effect of salinity and temperature on feeding physiology and scope for growth of an invasive species (*Brachidontes pharaonis* - Mollusca: Bivalvia) within the Mediterranean Sea. In *Journal of Experimental Marine Biology and Ecology* 363 (1), pp. 130–136. DOI: 10.1016/j.jembe.2008.06.030.

Schneider, A.; Wallace, D. W. R.; Körtzinger, A. (2007): Alkalinity of the Mediterranean Sea. In *Geophys. Res. Lett.* 34 (15). DOI: 10.1029/2006GL028842.

Schwabe, E.; Försterra, G.; Häussermann, V.; Melzer, R. R.; Schroedl, M. (2006): Chitons (Mollusca: Polyplacophora) from the southern Chilean Comau Fjord, with reinstatement of *Tonicia calbucensis* plate, 1897. In *Zootaxa* 1341 (1), pp. 1–27.

Sheppard, C. R. C.; Davy, S. K.; Piling, G. M. (2009): The Biology of Coral Reefs. The Abiotic Environment.

Shin, Y.-K.; Jun, J.-C.; Im, J.-H.; Kim, D.-W.; Son, M.-H.; Kim, E.-O. (2011): Physiological responses in abalone *Haliotis discus hannai* with different salinity. In *The Korean Journal of Malacology* 27 (4), pp. 283–289.

Shivakumar, K.; Jayaraman, J. (1986): Salinity adaptation in fish: interaction of thyroxine with fish gill mitochondria. In *Archives of Biochemistry and Biophysics* 245 (2), pp. 356–362.

Silva, N. (2008): 3.2 dissolved oxygen, ph, and nutrients in the austral chilean channels and fjords. In *Progress in the oceanographic knowledge of Chilean interior waters, from Puerto Montt to Cape Horn*, p. 37.

Sokol, S. (2012): The influence of heterotrophy and flow on calcification of the cold-water coral *Desmophyllum dianthus*: University of Kiel, AWI.

Somero, G. N.; Yancey, P. H. (1997): Osmolytes and cell volume regulation: physiological and evolutionary principles. In *Handbook of physiology*, pp. 441–484.

Sorauf, J. E.; Jell, J. S. (1977): Structure and incremental growth in the ahermatypic coral *Desmophyllum cristagalli* from the North Atlantic.

Svetlichny, L.; Khanaychenko, A.; Hubareva, E.; Aganesova, L. (2012): Partitioning of respiratory energy and environmental tolerance in the copepods *Calanipeda aquaedulcis* and *Arctodiaptomus salinus*. In *Estuarine, Coastal and Shelf Science* 114, pp. 199–207.

Tam, T.; Ang Jr, P. O. (2008): Repeated physical disturbances and the stability of sub-tropical coral communities in Hong Kong, China. In *Aquatic Conservation: Marine and Freshwater Ecosystems* 18 (6), pp. 1005–1024.

Taviani, M.; Angeletti, L.; Canese, S.; Cannas, Rita; Cardone, F.; Cau, Angelo et al. (2017): The “Sardinian cold-water coral province” in the context of the Mediterranean coral ecosystems. In *Deep Sea Research Part II: Topical Studies in Oceanography* 145, pp. 61–78.

Taviani, M.; Freiwald, A.; Zibrowius, H. (2005): Deep coral growth in the Mediterranean Sea: an overview. In *Cold-water corals and ecosystems*, pp. 137–156.

Tedengren, M.; Kautsky, N. (1986): Comparative study of the physiology and its probable effect on size in Blue Mussels (*Mytilus edulis*) from the North Sea and the Northern Baltic Proper. In *Ophelia* 25 (3), pp. 147–155. DOI: 10.1080/00785326.1986.10429746.

Thiem, Ø.; Ravagnan, E.; Fosså, J. H.; Berntsen, J. (2006): Food supply mechanisms for cold-water corals along a continental shelf edge. In *Journal of Marine Systems* 60 (3-4), pp. 207–219.

van Oevelen, D.; Duineveld, G.; Lavaleye, M.; Mienis, F.; Soetaert, K.; Heip, C. H. R. (2009): The cold-water coral community as hotspot of carbon cycling on continental margins: A food-web analysis from Rockall Bank (northeast Atlantic). In *Limnology and Oceanography* 54 (6), pp. 1829–1844.

van Woesik, R.; Vantier, L. M. de; Glazebrook, J. S. (1995): Effects of Cyclone 'Joy' on nearshore coral communities of the Great Barrier Reef. In *Marine Ecology Progress Series* 128, pp. 261–270.

Van't Hoff, J. H.; van Deventer, C. M. (1886): Ueber die Umwandlungstemperatur bei chemischer Zersetzung. In *Berichte der deutschen chemischen Gesellschaft* 19 (2), pp. 2142–2153.

White, M.; Bashmachnikov, I.; Arístegui, J.; Martins, A. (2007): Physical processes and seamount productivity. In *Seamounts: ecology, fisheries and conservation*, pp. 65–84.

Widdows, J. (1985): The effects of fluctuating and abrupt changes in salinity on the performance of *Mytilus edulis*: J Wiley, Chichester. In *Marine biology of polar regions and effects of stress on marine organisms*.

Wild, C.; Mayr, C.; Wehrmann, L.; Schöttner, S.; Naumann, M.; Hoffmann, F.; Rapp, H. T. (2008): Organic matter release by cold water corals and its implication for fauna–microbe interaction. In *Marine Ecology Progress Series* 372, pp. 67–75.

Xiubao, L.; Hui, H.; Jiansheng, L.; Liangmin, H.; Junde, D. (2009): Effects of the multiple stressors high temperature and reduced salinity on the photosynthesis of the hermatypic coral *Galaxea fascicularis*. In *Acta Ecologica Sinica* 29 (3), pp. 155–159.

Yu, Z.; Qi, Z.; Hu, C.; Liu, W.; Huang, H. (2013): Effects of salinity on ingestion, oxygen consumption and ammonium excretion rates of the sea cucumber *Holothuria leucospilota*. In *Aquaculture Research* 44 (11), pp. 1760–1767.

## 9 Supplementary materials

Table-- S2 *D. dianthus* growth analysis regarding environmental parameters, applying Spearman correlation, expressed in correlation coefficient  $\rho$  and related p-value: salinity, temperature [°C], pH, oxygen [mg L<sup>-1</sup>], NO<sub>3</sub><sup>-</sup> [μmol kg<sup>-1</sup> SW], NO<sub>2</sub><sup>-</sup> [μmol kg<sup>-1</sup> SW], NH<sub>4</sub><sup>+</sup> [μmol kg<sup>-1</sup> SW], PO<sub>4</sub><sup>+</sup> [μmol kg<sup>-1</sup> SW], and  $\Omega_{arag}$ , occurring during acclimation and the experimental phase.

	Acclimation		Experiment	
	$\rho$	p-value	$\rho$	p-value
<b>S</b>	0.75	< 0.01	0.71	< 0.01
<b>T</b>	0.28	0.38	-0.04	0.84
<b>pH</b>	0.41	0.18	0.43	0.03
<b>O<sub>2</sub></b>	0.15	0.64	-0.33	0.09
<b>NO<sub>3</sub><sup>-</sup></b>	-0.37	0.24	< 0.01	0.98
<b>NO<sub>2</sub><sup>-</sup></b>	0.30	0.35	0.09	0.66
<b>NH<sub>4</sub><sup>+</sup></b>	-0.09	0.78	0.25	0.22
<b>PO<sub>4</sub><sup>-</sup></b>	0.07	0.82	0.04	0.85
<b><math>\Omega_{arag}</math></b>	0.71	< 0.01	0.60	< 0.01